

1 February 1967


FINAL REPORT
STUDIES OF
EXTRATERRESTRIAL DUST
AT 40 KILOMETERS
(1966)

Contract NASW-1395

Prepared for:


National Aeronautics and Space Administration
Washington, D. C. 20546

Approved by:


R. C. Wood, Manager
Upper Air Programs

Prepared by:

R. Wood
H. Zeller
R. Olson
R. Deeter
K. Maffitt
H. Anderson


A. A. Anderson, Director
Research and Development

Report No. 3063
Project No. 57014

APPLIED SCIENCE DIVISION
Litton Systems, Inc.
2003 East Hennepin Avenue
Minneapolis, Minnesota 55413

TABLE OF CONTENTS

Section	Title	Page
1	Introduction and Summary	1
2	Characteristics of the Collection System	4
3	Preparation of the Collection Surfaces	10
4	Steps to Minimize Contamination	14
5	Sample Acquisition at 40 Kilometers	17
6	Post-Flight Evaluation of Sample Integrity	17
7	Electron Microscope Studies	21
8	Particle Analysis by Nuclear Magnetic Resonance	31
9	Particle Studies with the Electron Mirror Microscope	34
10	Electron Microprobe Analysis	51
11	Discussion of Results	52

LIST OF ILLUSTRATIONS

Figure	Title	Page
1	Jet Impactor System	5
2	Air Ejector Pump	7
3	Air Ejector Impactor Sampler	9
4	Auxiliary Lift Balloon and Sampler	18
5	Time-Altitude Profile of Flight 3036	19
6	Typical Particle Field on Pre-Shadowed Grid	22
7	Typical Field Showing Single Large Contaminant Particle	23
8	Typical Field, Oil-Coated Grid	24
9	Oil-Coated Grid after Shadowing with Chromium	25
10	Halo-Like Particle Produced by Exposure to Water Vapor	27
11	Particle Number Density as a Function of Distance Across the Collection Surface	29
12	Size Distribution of Particles Collected	30
13	Schematic of Y-Type Electron Mirror Microscope	35
14	EMM Microphoto of Flight Control Surface	40
15	EMM Microphoto, Center of Collection Area, Oil-Coated Slide	40
16	EMM Microphoto, Edge of Collection Area, Oil-Coated Slide	41

LIST OF ILLUSTRATIONS (Cont'd)

Figure	Title	Page
17	EMM Microphoto, Center of Impaction Area, Dry Slide	41
18	EMM Microphoto, Edge of Impaction Area, Dry Slide	42
19	Same Sample as Fig. 18; Particles Bombarded with 10 eV Pulses	42
20	Same Sample as Fig. 18; Particles Bombarded with 15 eV Pulses	44
21	Sample at 25 ⁰ C; Particles Bombarded with 40 eV Pulses	44
22	Sample at 90 ⁰ C; Particle Bombarded with 40 eV Pulses	45
23	Sample at 175 ⁰ C; Particles Bombarded with 40 eV Pulses	45
24	Sample at 224 ⁰ C; Particles Bombarded with 40 eV Pulses	46
25	Sample at 350 ⁰ C; Particles Bombarded with 40 eV Pulses	46
26	After Cooling Back to 25 ⁰ C; Particles Bombarded with 40 eV Pulses	47

STUDIES OF EXTRATERRESTRIAL DUST AT 40 KILOMETERS

1. Introduction and Summary

On 24 August 1966, a balloon-borne sampling probe was launched from a site near Minneapolis, Minnesota. Suspended at the end of a long nylon line 240 meters below the balloon, the 140 kg payload was lifted to an altitude of 42.6 km. During a sampling period of 5 hours and 20 minutes, an air ejector pump pulled approximately 12,000 m³ of air through a jet impactor particle collector. This flight was performed in support of a program to: (1) demonstrate the feasibility of acquiring large samples of extraterrestrial dust, and (2) explore the possibilities for particle analysis offered by new analytical methods.

Initial post-flight examinations of the sampler collection substrate revealed the presence of many submicron particles. These particles were concentrated in a sharply defined track that corresponded with the location of the impactor jet above the collection surface. Electron microscope grids mounted within the sampler cavity as flight controls were found to be relatively clean, with particles counts at least three orders of magnitude less than those found on exposed surfaces.

Studies performed with an Hitachi HU-11 electron microscope indicated that the sample consisted of optically dense irregular spheroids having a number mean diameter on the order of 0.1 micron. Subsequent tests indicated that these particles were very hydroscopic, a feature previously observed in stratospheric aerosols collected by other investigators (Junge, Chagnon and Manson, 1961).

Because of the small size of these particles and the absence of large, micron-size agglomerates, it was concluded that procedures taken to avoid reintrainment of contaminant particles from the payload or balloon surfaces were successful.

The particles were subjected to various analyses involving electron microscopy, electron mirror microscopy, NMR analysis, and electron microprobe analysis.

Electron micrographs analyzed statistically yielded a size distribution that was approximately log-normal, with a standard geometric deviation on the order of 1.8. Projections based on the total volume of air sampled and the number of particles collected, implied the existence of a particle number concentration at altitude (40 km) on the order of 250 particles per liter.

Studies of particle electrical properties by means of the electron mirror microscope indicated that virtually all(> 95%) of the particles were non-conductors. Differences in particle conductivity and response to electron bombardment tended to establish the existence of two major particle species. No particles having magnetic properties were detected.

NMR analysis revealed the presence of a definite complex spectra not present in control samples. Because of the small sample size, this spectra was poorly defined. It was not possible to identify molecular interactions associated with possible combinations of the more abundant elements.

The most significant analysis data was obtained late in the program using the electron microprobe analyzer located in the Geology Department of the University of Minnesota. Earlier attempts at microprobe analysis using "as collected" particles were not successful due to low mass of individual particles in the electron beam. Later in the program, a technique was developed for concentrating the particles to obtain a total mass sufficient for

microprobe analysis. The first examination under these conditions yielded positive evidence of three elements: potassium, chlorine and lead. A second examination, using a larger sample, confirmed this.

While it is not inconceivable that these elements could be present in the stratosphere, the absence of other more abundant elements such as sodium, iron, sulfur and silicon have led us to suspect that the particles may have originated from some contamination source. In view of this, a detailed re-examination of the flight payload was performed in an effort to identify such a source. In examining the sampler gondola, a small area of residue was found adjacent to the mounting bracket used to hold an explosive squib. This would indicate that gas leakage occurred when the squib was fired. Communications from the squib manufacturer relative to charge composition revealed that the proprietary formulation included potassium chlorate and lead nitrate.

It should be pointed out that this squib actuator normally functions as an emergency device to cut the gas line and depressurize the gas cylinder in the event that a premature balloon burst necessitates command separation of the payload. On a normal flight, where the sequence of events is controlled by an automatic programmer, this device would have fired about 10 minutes after the sampler closed.

In this instance however, a projected track for the full 7 hours placed the payload impact in a populated area. To avoid this, the payload was released by radio-command approximately 1-1/2 hours ahead of schedule. Under command termination, the explosive squib fired to cut the gas supply line at the instant of release. With the gas supply cut off, the ejector pump stopped and the sampler automatically closed. Although the consequences of this act were not foreseen, it appears from subsequent analyses that combustion products were ingested during the few seconds between squib actuation and sampler closure.

As a result of this circumstance, it is evident that the various analyses performed can not be considered a reliable source of information relative to stratospheric or extraterrestrial dust. This work, involving electron microscopy, electron mirror microscopy, and nuclear magnetic resonance, was performed before the electron microprobe data became available. Results are included principally as a matter of interest and for the sake of completeness.

2. Characteristics of the Collection System

Design of a sampling system suitable for the collection of extraterrestrial dust has involved the application of principles and techniques developed over the past few years in connection with stratospheric sampling programs. These have been treated extensively in other scientific publications (Stern et al., 1962; Chagnon and Junge, 1961; McFarland and Zeller, 1963; Wood, 1966), but it may be appropriate to include a brief description of the principles involved for completeness.

The sampler used in this program consists basically of a slit impactor coupled to an air ejector pump. In operation, particle-laden air is pulled through an appropriately designed slit orifice as shown in Fig. 1. An impactor plate located downstream from the slit causes the air streamlines to bend sharply while the particle's inertia tends to keep moving it toward the plate. If the particle inertia is sufficiently high, it will impact on the collection plate.

The collection efficiency of a jet impaction system is characterized by

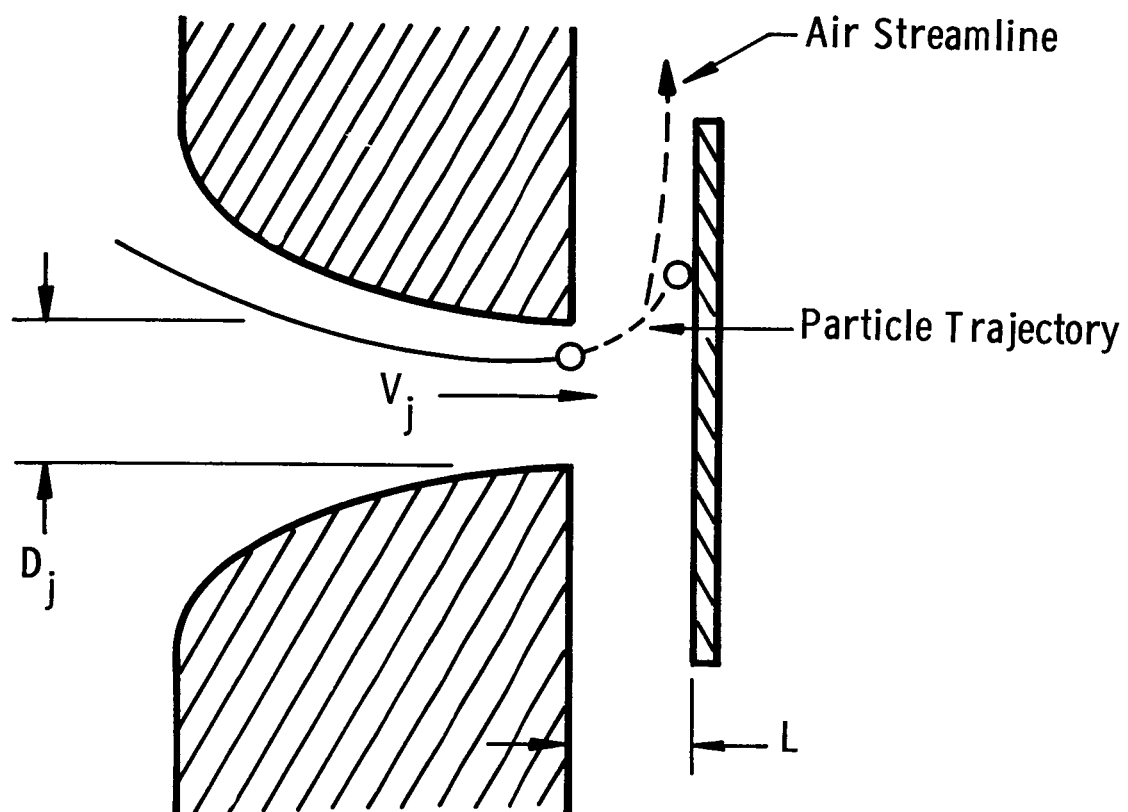


Fig. 1. Jet Impactor System

the value of an inertial parameter K where

$$K = \frac{C \rho_p V_j D_p^2}{18 \mu_j D_j} \quad (1)$$

and, C = Cunningham's slip correction,

ρ_p = Particle density

V_j = Jet air velocity,

D_p = Particle diameter,

μ_j = Jet air viscosity,

D_j = Jet (slit) width.

Other variables which must also be considered are the Jet Reynolds number, Re_j ; the jet clearance, L, and the inlet shape. The collection efficiency, η , in functional notation, neglecting the shape factor, is then expressed by:

$$\eta = (K, Re_j, L/D_j). \quad (2)$$

Theoretical solutions for this equation have been developed by a number of investigators (Ranz and Wong, 1952; Davies and Aylward, 1951). In general, however, experimental methods have been employed to obtain data from which performance characteristics may be accurately predicted.

Since impactor design involves factors which include air density, flow rate, and pressure drop, it is obvious that performance characteristics of the air mover must be considered. For this application, we have selected an air ejector pump developed for the U. S. Atomic Energy Commission in connection with a program to sample radioactive, stratospheric debris. Basically, an air ejector pump is a simple device. As illustrated in Fig. 2, a jet of high-velocity primary gas injected into a mixing tube will expand to entrain the surrounding

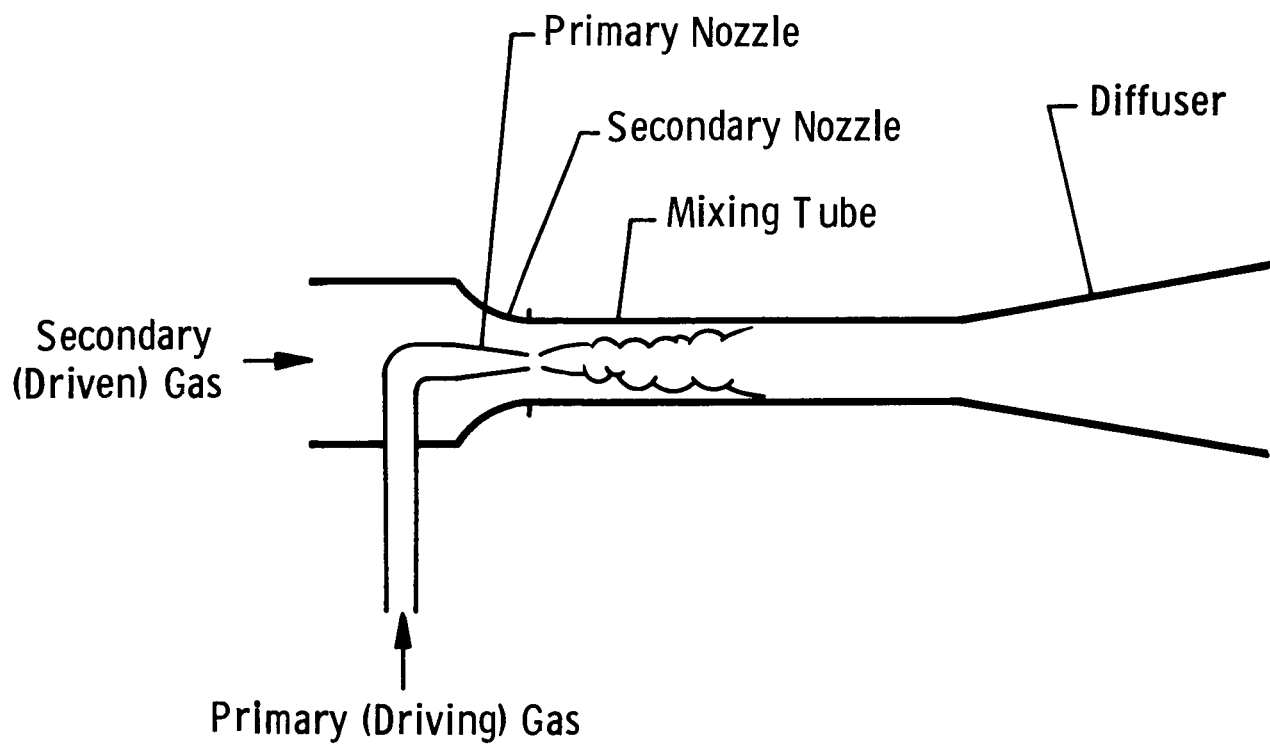


Fig. 2. Air Ejector Pump

secondary air. The resulting turbulent exchange of momentum between the driving (primary) gas and the driven (secondary) air produces a region of reduced pressure and a net flow through the system.

Theoretical calculations supported by performance data acquired in operational use, have indicated that an ejector pump-slit impactor combination could be designed to operate at 40 km. The system illustrated in Fig. 3 has the physical and performance characteristics given in Table 1.

Table 1. Characteristics of the Large Volume Impactor Sampler at 40 km (Nominal).

Sampling rate	30m ³ /min
Particle size cutoff, diameter*	0.1 micron
Impactor slit width	3 mm
Impactor slit length	400 mm
Number of impactor slits	8
Total area, particle deposit	96 cm ²
Compressed nitrogen "fuel"	50 lb
System weight at launch**	350 lb

*Lower limit at which collection efficiency becomes 50% for spherical particles of unit density.

**Includes peripheral instrumentation, ballast, suspension cable.

As shown in the diagram (Fig. 3) the collection head consists of eight slit impactors arranged around the periphery of a 6-inch cylinder. This assembly is exposed and retracted by means of a linear pneumatic actuator. Because it is connected to the primary gas supply, the actuator (a spring-loaded piston) exposes the collector head automatically when the system programmer commands the air ejector to start the sampling period. The collector retracts when the sampler is turned off or the nitrogen becomes exhausted. Four

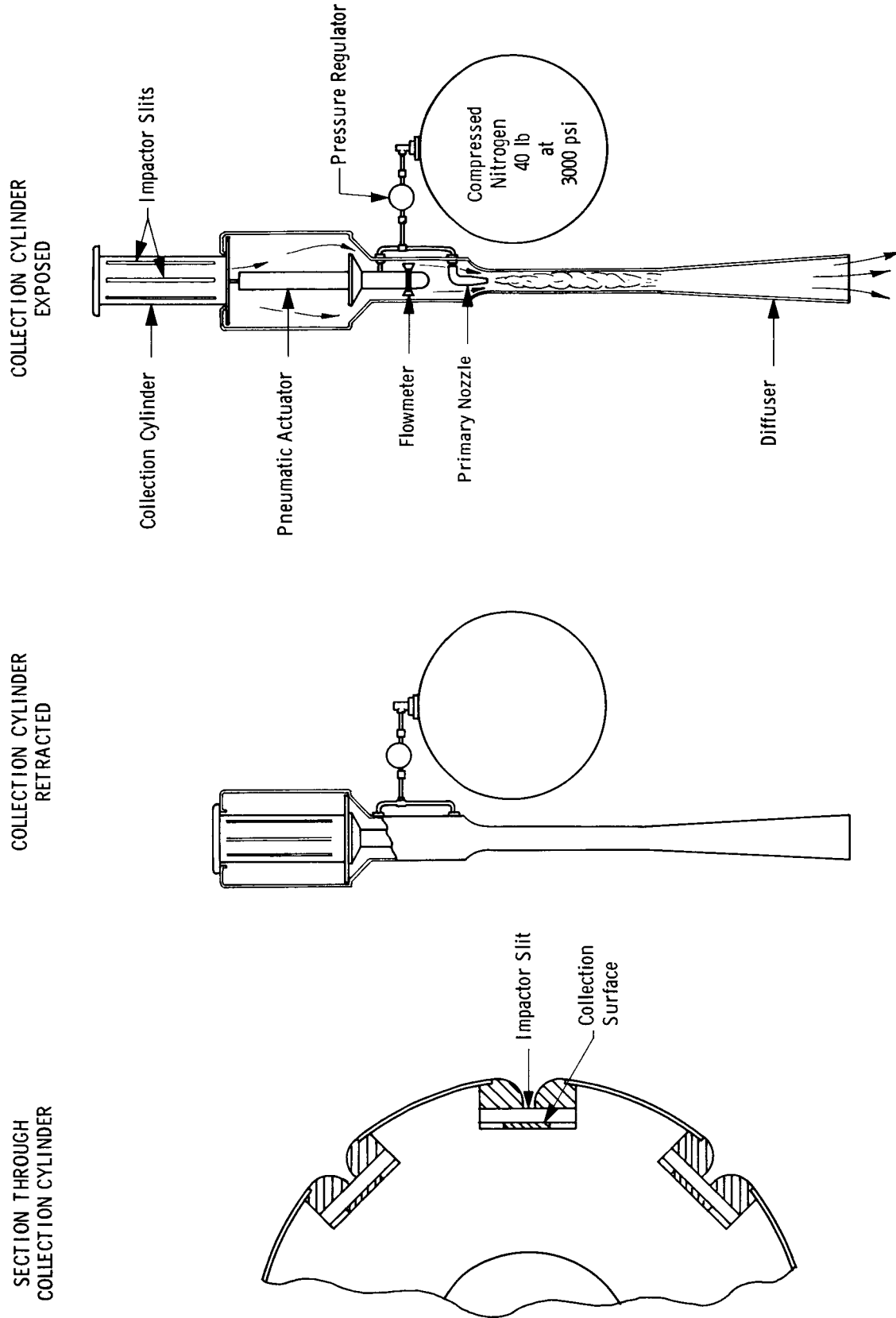


Fig. 3. Air Ejector Impactor Sampler

spring-loaded latches actuated at 90,000 feet by a pressure switch, serve to prevent the sample container from being jarred open at the landing impact.

Although the system incorporates very tight, secure closures, it is extremely difficult to achieve a true hermetic seal that would effectively prevent the entry of water vapor during descent. In view of this, a vent has been provided to allow pressure equalization through a small desiccant chamber backed up by two membrane filters.

Collection surfaces are mounted within the sampling head on eight aluminum backing strips. These numbered strips are positioned accurately behind each impactor slit and held firmly in place by locking pins. The prepared surfaces are installed and removed through the top of the sampler.

3. Preparation of the Collection Surfaces

The primary analysis procedures employed in this work have imposed different requirements with respect to the substrate upon which the particles are impacted. In view of this, three basic types of collection surfaces were prepared:

- 1) Electron microscope, - formvar film on copper grid,
- 2) Electron mirror microscope, - gold on microscope cover slip,
- 3) Nuclear magnet resonance spectrometer, - strippable plastic film on glass slide.

Within each basic type of collector, there were also some differences in surface preparation as noted in the following description of the fabrication methods employed.

Electron Microscope Grids

The sampler carried a total of 50 electron microscope grids. Forty of these were used for sample collection; ten as flight controls:

Exposed Grids:		Quantity
Type 1.	Dry Formvar film	20
Type 2.	Formvar film, chromium pre-shadow	10
Type 3.	Formvar film, 0.1-micron oil overlay	10
Flight Controls:		
Type 1.	Dry Formvar film	5
Type 3.	Formvar film, 0.1-micron oil overlay	5

The basic, Type 1 grids, consisted of a Formvar film supported by 200-mesh copper screens, 3 mm in diameter. The film was cast on a clean microscope slide by dipping the slide into a 0.50 percent solution of Formvar in ethylene dichloride. After drying, the film was floated from the slide onto a distilled water surface. Copper screens dropped on the floating film were then picked up with a second microscope slide. Slides with film-covered screens attached were placed in petri dishes and stored in a clean box until needed.

The Type 2, pre-shadowed grids were prepared by evaporating a thin deposit of chromium from a source elevated approximately 15° above the grid surface. Because these grids were re-shadowed after the flight, they provided means for identification of contaminant particles (double shadows) acquired during grid preparation.

Type 3 grids were prepared by dipping and slowly withdrawing the grid holder from a 0.3% solution of 100,000-centistoke Dow Corning silicone oil diluted in spectral-purity hexane. The resulting film, approximately 0.1 micron thick, was reasonably transparent to the microscope electron beam and provided a tacky surface for particle retention. A comparison of particle counts on the dry- and oil-coated grids provided information relative to the particle loss from dry surfaces due to bounce-off.

Electron Mirror Microscope Gold Surfaces

The sampler carried a total of 30 gold substrates deposited on 25-millimeter, circular glass cover slips. Twenty-four of these were used for sample collection; ten as flight controls:

Exposed Surfaces:		Quantity
Type 4.	Dry gold film	8
Type 5.	Gold film, 0.1-micron oil overlay	8
Type 6.	Gold film, 0.5-micron oil overlay	8
Flight Controls:		
Type 4.		2
Type 5.		2
Type 6.		2

The basic, Type 4 surface was prepared by evaporating a gold film over the surface of glass microscope cover slips. Prior to evaporation, the glass discs were cleaned ultrasonically in a detergent solution, rinsed in distilled water, and exposed to hot iso-propanol vapor in a reflux bath. The evaporation

chamber was cleaned and its inside surfaces were coated with a low vapor pressure grease to trap and hold dust particles. As a further precaution, the sample rack was mounted above the evaporation source so that falling dust particles would tend to collect on the back side of a slide, not on the gold surface. The system was pumped down at a slow rate and, after the evaporation process, the chamber was returned to atmospheric pressure by admitting air through a membrane filter.

Type 5 and Type 6 substrates consisted of the basic Type 4 surface to which a thin silicone oil film had been added. Film thicknesses of 0.1 micron (Type 5) and 0.5 micron (Type 6) were achieved by dipping the prepared cover slips in 0.3% and 1.5% solutions of 100,000 centistoke silicone oil diluted in spectral purity hexane.

Strippable Plastic Films for NMR Analyses

Fourteen glass slides, 220 mm long and 12 mm wide served to support the strippable plastic films upon which the sample for NMR (Nuclear Magnetic Resonance) analysis was collected. Twelve of these slides were used for sample collection; two as flight controls:

Exposed Surfaces		Quantity
Type 7.	Dry plastic film	6
Type 8.	Plastic film, 0.5-micron oil overlay	6
Flight Controls:		
Type 7.		1
Type 8.		1

As a base for the Type 7 surface, the glass slides were cleaned thoroughly using methods previously described. The thin plastic film substrate was prepared

using a formulation* developed for the U. S. Atomic Energy Commission in previous similar work. After application to the glass slide base, the surfaces were allowed to dry thoroughly in a dust-free, laminar flow box. The completed films, approximately 35 microns thick were strong and relatively easy to strip from the glass surface. Type 8 films were prepared by adding an 0.5-micron oil overlay to the basic Type 7 surface in the manner previously described.

4. Steps to Minimize Contamination

Background interferences stemming from many potential sources of contamination probably constitute the most important problem in this work. These sources include:

- 1) Impurities in the collection substrate,
- 2) Airborne terrestrial particulates,
- 3) Dust on internal and external sampler surfaces, gondola framework, loadlines,
- 4) Particles in the primary gas supply,
- 5) Dust from the balloon,
- 6) Condensable vapors from batteries, and explosive actuators.

Impurities in the collection substrate constitute a potential source of interference in connection with analyses involving nuclear magnetic resonance, electron microprobe, and neutron activation. For this reason, extreme care in the cleaning and handling of the various substrates was felt necessary. Strip-pable films were prepared using reagents and chemicals of high purity; some constituents were re-distilled; all liquids were processed through membrane

*One part dibutyl phthalate, ten parts cellulose acetate butyrate, 90 parts cyclo-hexanone.

filters. Prior to the application of films, glass substrate supports were cleaned ultrasonically in a detergent solution, rinsed in distilled water, immersed in chromic acid, rinsed in distilled water, and treated in an iso-propanol hot vapor reflux bath. Strippable films were applied in a Dexon "Primaire" dust-free laminar flow box.

Contamination due to the normal diffusion of airborne dust was effectively minimized by enclosing the sampling head within a tightly sealed aluminum housing. The entire housing assembly was protected by a rigid plastic shroud jettisoned during ascent at 90,000 feet.

The secondary reintrainment of dust during the sampling process, was minimized by coating all internal and external sampler surfaces, shroud, gondola, and load line with silicone oil. To guard against the possible recirculation of particulates ejected with the primary gas "fuel", the supply line incorporated a small particulate filter upstream of the primary exhaust nozzle.

Normally, the most important potential source of contamination on a flight of this type is the 6-acre expanse of polythelylene film presented by the balloon. Since it is obviously impossible to manufacture, inflate, and launch such a vehicle without acquiring some burden of dust, we have attempted to reduce contamination from this source by providing 240 meters (800 feet) of separation between the balloon and the sampler.

The effectiveness of this arrangement depends mainly upon the existence and magnitude of a local wind shear at sampling altitude. In viewing this situation with respect to contaminant particles smaller than 5 microns, it is evident that particle fall velocity is small compared to the magnitude of vertical balloon motions possible during the sampling interval. Neglecting particle motion, it is possible to develop an approximate relationship between ascent rate and the shear required (Table 2) in order to avoid balloon contamination.

Table 2. Wind Shear Required to Prevent Sampling
of Dust from Balloon Surfaces.

Given: Balloon Radius		46 meters
Vertical separation, center of balloon to payload		300 meters
Capture radius of sampler (0.1 μ particle)		10 meters
ASCENT RATE (Meters/min)	HORIZONTAL TRANSLATION (Meters)	WIND SHEAR REQUIRED (Meters/min/300 meters)
5	56	0.9
10	56	1.9
15	56	2.8
20	56	3.7
25	56	4.7

Other miscellaneous potential sources of contamination, including batteries and actuators, were given attention. Batteries for the radio link, data recorder and squib operation were hermetically sealed types without vents. Explosive squibs used for ballast drop, shroud jettison and sampler latching, were of a sealed type designed to retain smoke and gases. The arrangement of these units and the firing sequence employed was such as to minimize the change of contamination should any leakage occur. Size considerations dictated the use of one open squib to function as an emergency gas dump valve (pneumatic line cutter) in the event a premature balloon burst would necessitate a command payload release. On a normal flight this unit would be fired by the on-board programmer, approximately 10 minutes after the sampler had closed.

5. Sample Acquisition at 40 Kilometers

Launch of the NASA sampling probe (Fig. 4) was accomplished without incident at 0630 CST, 24 August 1966, from a site located a few miles north-east of Minneapolis, Minnesota. At 0847 CST (27 km), a pressure switch actuated to remove the protective dust cover from the sampler. At 1048 CST (42 km), the system programmer extended the sampling head outside its container and activated the air ejector pump. After a sampling interval of 5 hours and 20 minutes, the flight was terminated by radio command. The payload descended by parachute. The recovery crew reached the payload with a few minutes of impact and found the sampler in good condition, securely closed and locked. The time-altitude profile is shown in Fig. 5; performance data are summarized in Table 3.

Table 3. Sampler Performance, Flight 3036

Maximum sampling altitude	43.5 km
Minimum sampling altitude	41.2 km
Average sampling altitude	42.6 km (139,800 ft)
Average sampling rate*	36.6 m ³ /min (1200 ft ³ /min)
Sampling interval	320 min
Total volume processed*	11,700 m ³ (410,000 ft ³)

*These values are derived from experimental pump performance data and should have an uncertainty no greater than $\pm 20\%$.

6. Post-Flight Evaluation of Sample Integrity

After recovery, a post-flight evaluation was performed to determine if a valid, usable sample had been collected. The sampler head was opened in a dust-free, laminar-flow hood and individual support slides were placed in clean

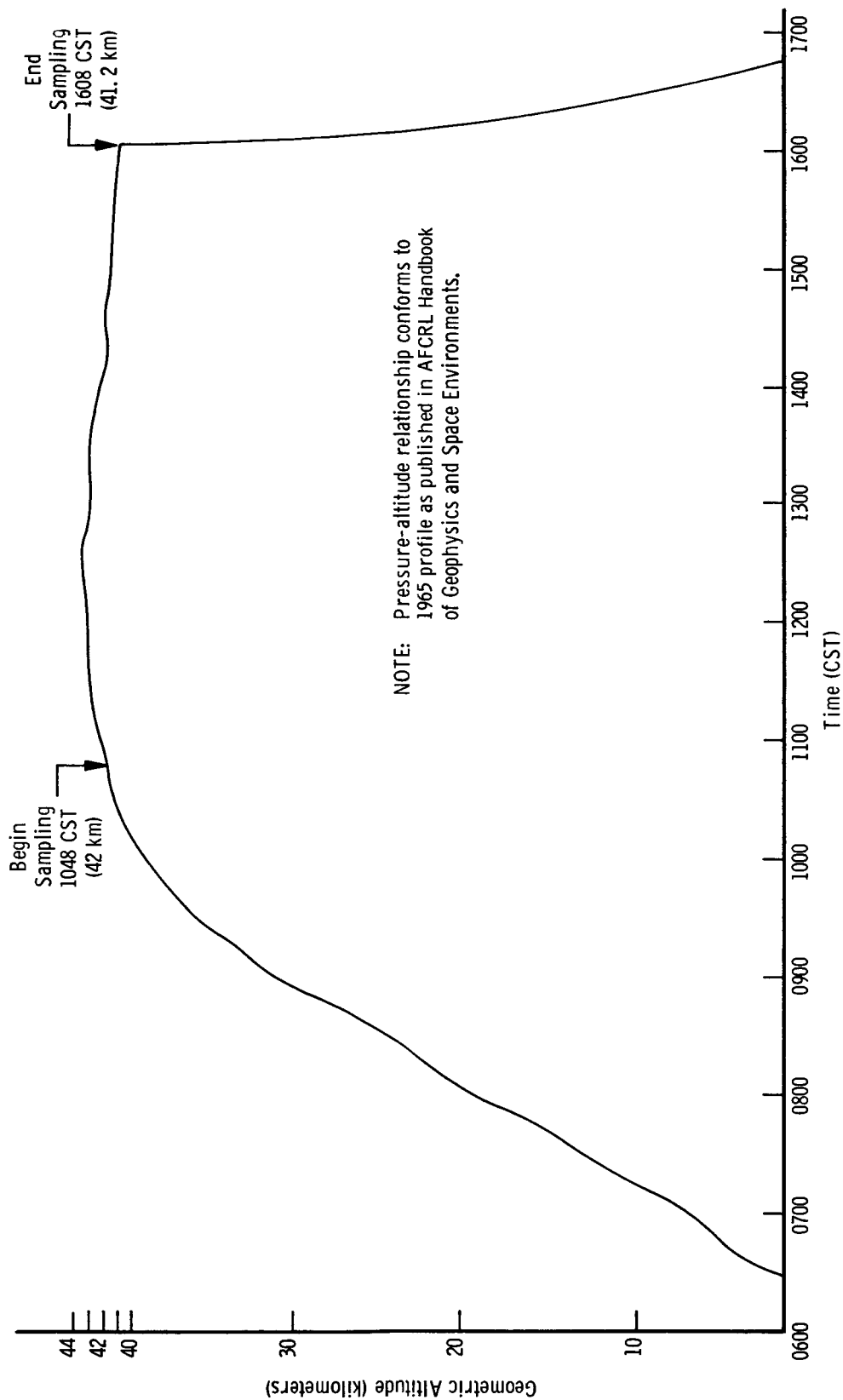


Fig. 5. Time-Altitude Profile of Flight 3036

glass tubes. During this process it was noted that a faint haze could be observed down the center of the gold-coated microscope cover slips. This track corresponded with the location of the impactor slit over the substrate surface and gave early indication that the sampler had collected particles.

This was quickly confirmed by a preliminary examination of electron microscope grids which revealed the presence of many submicron-size, irregular spheroids. Electron microscope grids attached within the sampler as flight controls were found to be relatively clean, with particle counts at least three orders of magnitude less than found on the exposed grids. This was generally consistent with the low number of double-shadowed contaminant particles found on pre-shadowed (Type 2) grids. It was concluded on the basis of this evidence, that the sampler closures functioned properly, and effectively prevented the entry of contamination during launch and recovery.

With respect to the possibility of contamination from the balloon, analysis of the flight profile indicated that the maximum rate of rise during the sampling interval (18 meters/min) occurred at the start of the sampling period at an altitude of 42 km. Winds-aloft data were not available at that altitude, but visual observations of the balloon through a theodolite gave indication of a track curvature apparently caused by wind gradients that probably exceeded the small value of 3.5 meters per minute per thousand feet required to avoid balloon contamination (ref. Table 2). This conclusion was reinforced by evidence stemming from the nature of the collected sample. Virtually all of the particles were in the sub-micron size range. In view of the strong (Van der Waals) forces between a particle and a surface, one would expect that contamination shaken loose from the balloon, or reentrained from nearby sampler surfaces must include particles of micron size or larger. Particles or agglomerates of this size were not observed. On the basis of the post-flight evaluation it was concluded that the collected sample was predominately of stratospheric or extraterrestrial origin, and that further detailed analyses were warranted.

7. Electron Microscope Studies

General Observations

A representative micrograph of particles collected on Flight 3036 is shown in Fig. 6. This view through a pre-shadowed (Type 2) grid typically shows no double-shadowed contaminant particles. Although such particles were searched for and found (Fig. 7), their rarity is evidenced by the fact that it was possible to count about 1400 particles in 11 random fields without observing a double-shadowed particle.

Particles collected on Type 1 (Formvar), and Type 2 (Formvar, pre-shadowed) screens, were generally similar in appearance and number density. Examination at 50 kv revealed many optically dense particles, generally spheroidal in shape. There were no loose fluffy agglomerates, no particles surrounded by rings or satellites, and no evidence of particle evaporation in the electron beam. The shape and length of the shadows indicate that the particles tended to remain spherical after impact; there was no evidence pointing to particle deformation or breakup.

A typical field from a Type 3 (oil-coated, unshadowed) screen is shown in Fig. 8. Although the 0.1-micron oil surface produced diffuse particle outlines, it is apparent that particle area concentration and size were about the same as observed on the dry screens.

In an attempt to enhance resolution and contrast, several of the oil-coated screens were shadowed at 15° with chromium. This produced rather striking results as shown in Fig. 9. An interesting feature made visible by the shadowing process is the slightly raised irregular plateau surrounding the larger particles. It is our opinion that terrestrial water vapor acquired after collection may be

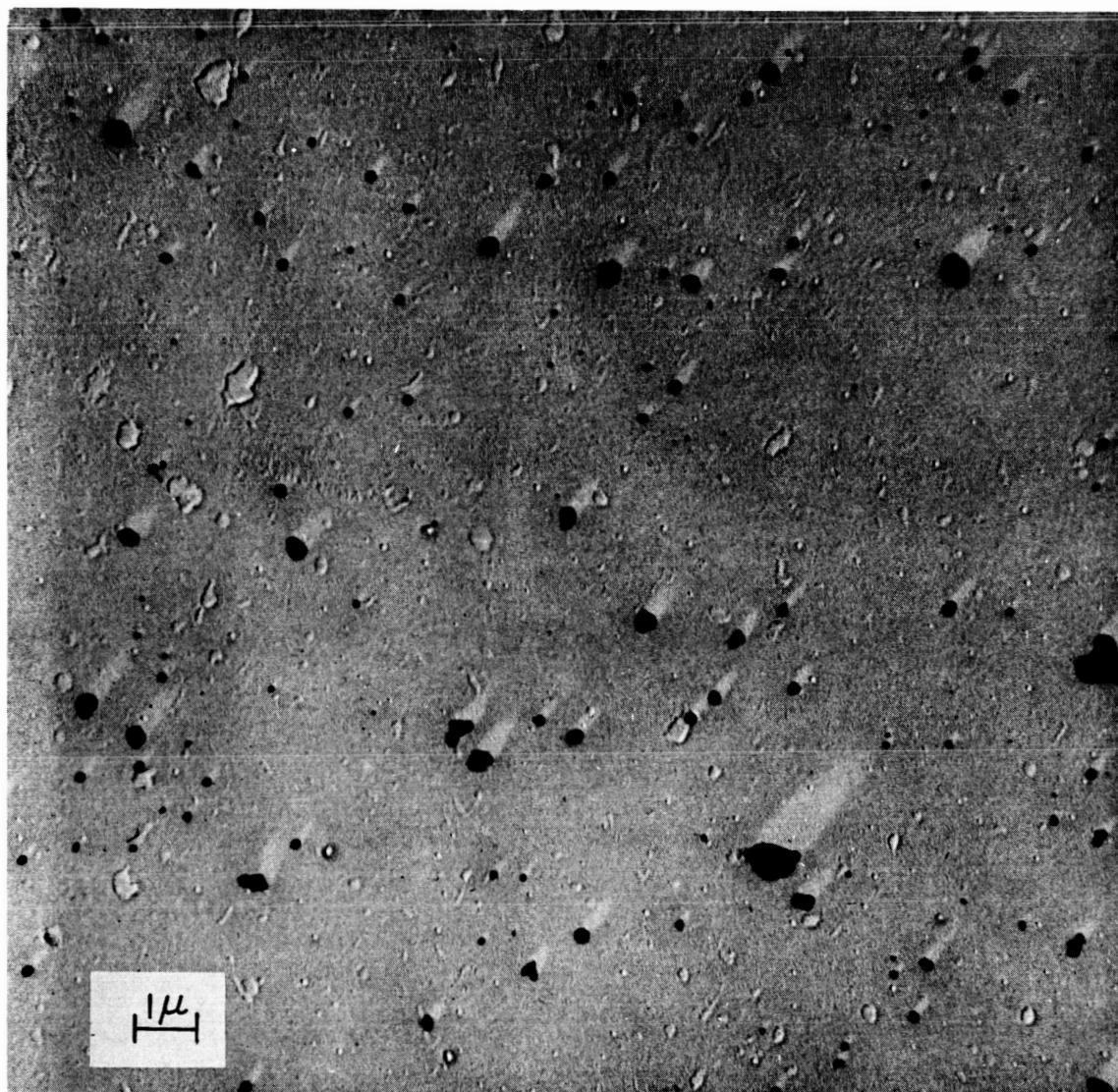


Fig. 6. Typical Particle Field on Pre-Shadowed Grid

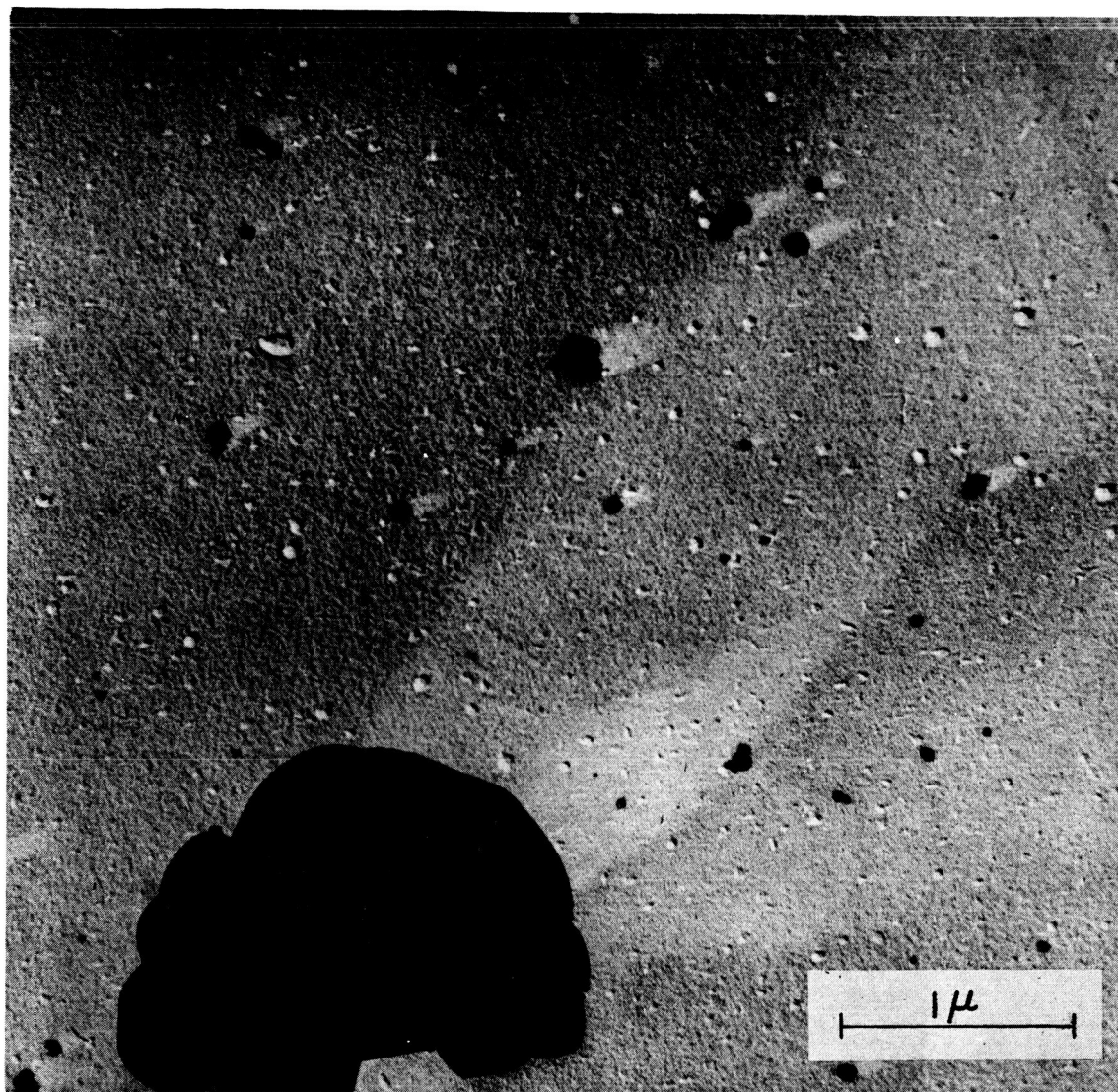


Fig. 7. Typical Field Showing Single Large Contaminant Particle



Fig. 4. Auxiliary Lift Balloon and Sampler

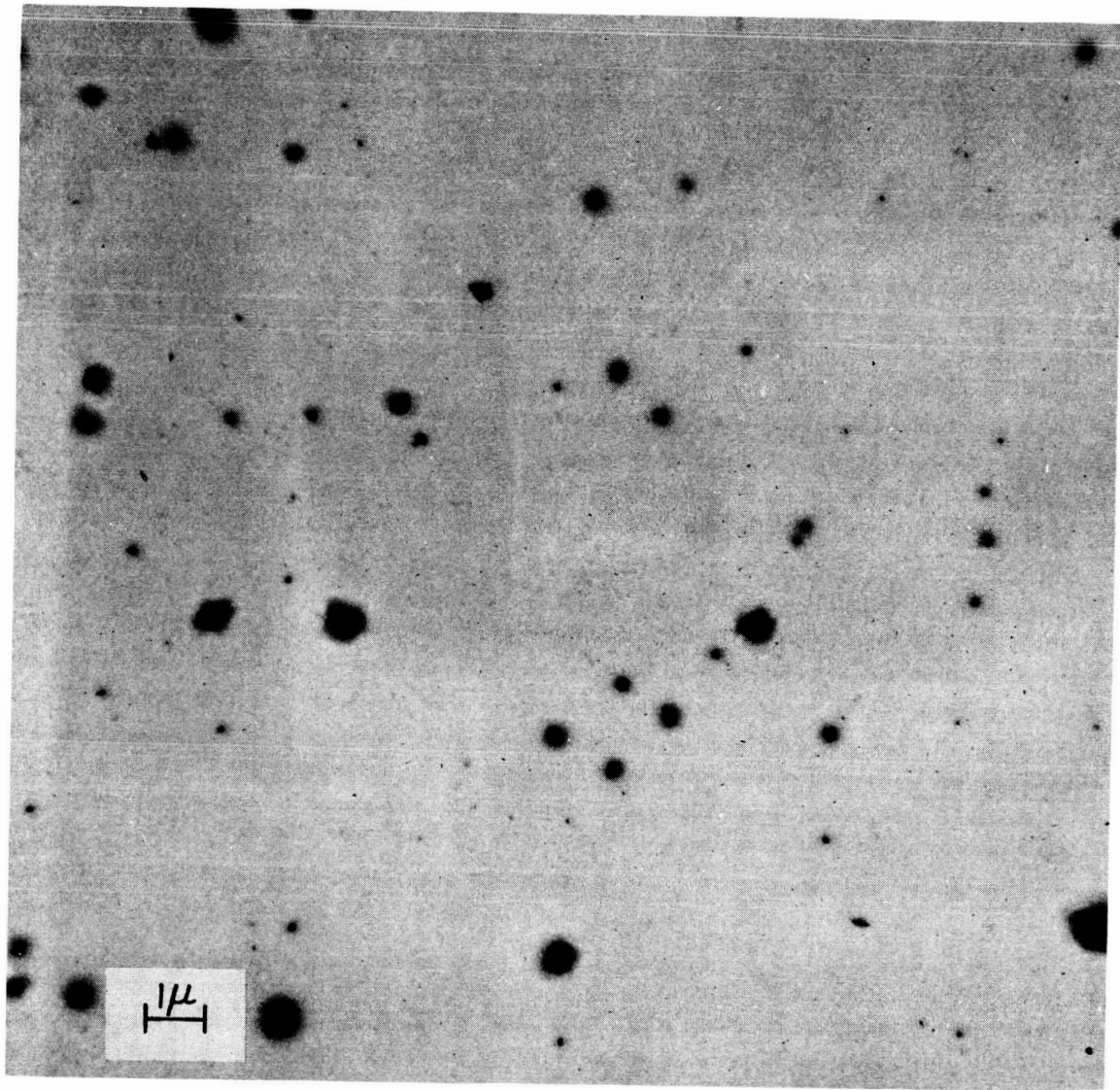


Fig. 8. Typical Field, Oil-Coated Grid

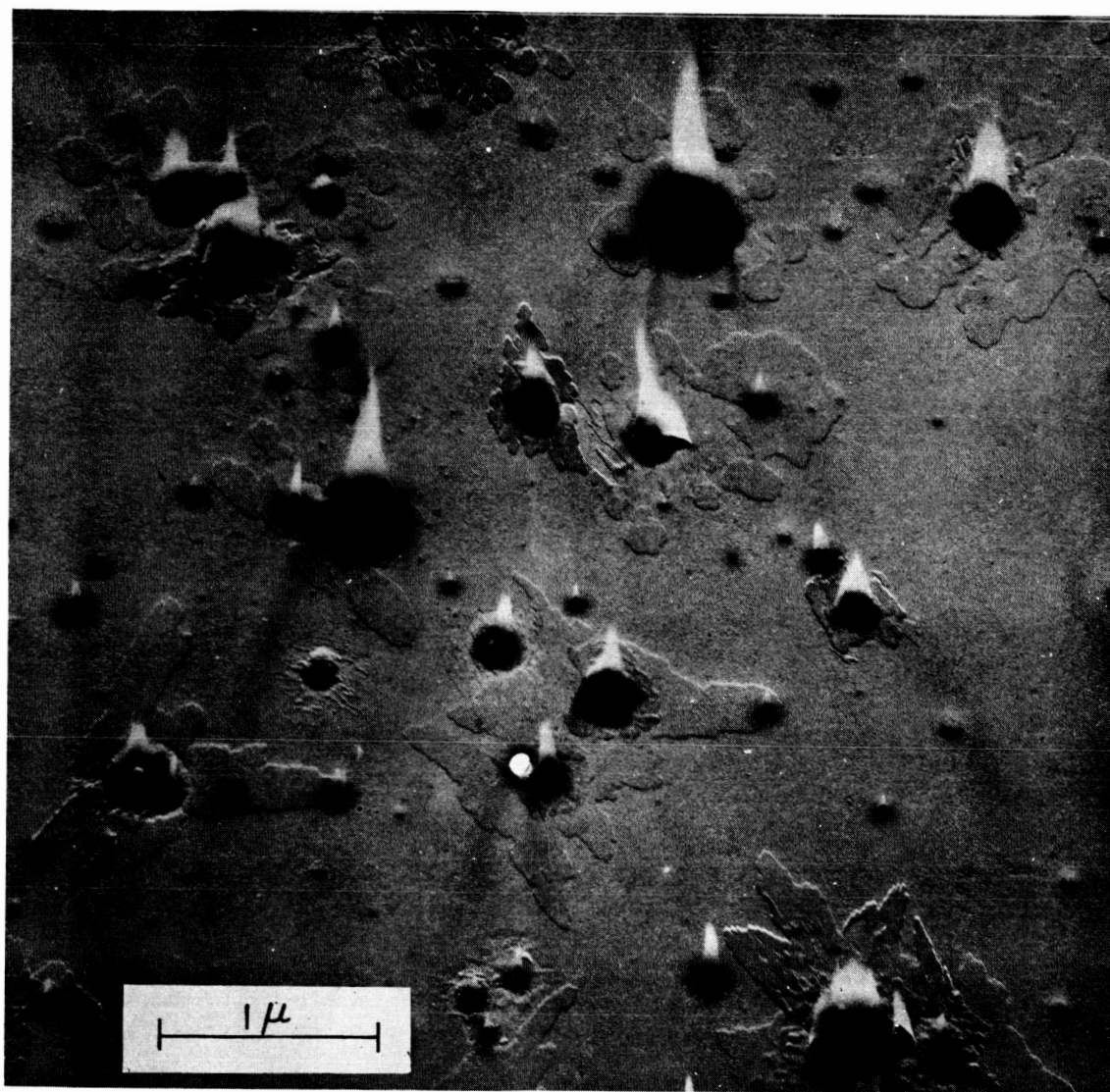


Fig. 9. Oil-Coated Grid after Shadowing with Chromium

a contributing factor in producing this apparent interaction between the collection surface and the particle. Evidence pointing to this stems from the fact that smaller particles, completely immersed in the oil overlay, have not produced similar patterns.

Hydroscopic Nature of the Particles

Because of precautions taken to exclude terrestrial water vapor from the sampler, plus the fact that initial studies of the collected sample were conducted soon after recovery, it is felt that the particles shown in Fig. 6 substantially represent the shape and appearance of the particle population at the time of collection.

With the progression of time, however, re-examination of these same grid screens has yielded unmistakable evidence of a change in particle size and appearance. Although stored in a 'particle free' environment, the screens were exposed to ambient humidity conditions particularly in the laminar flow clean box, the shadow casting apparatus, and in the electron microscope. Apparently as a result of particle hygroscopicity, small but continuous changes in particle properties resulted. The most obvious changes involved deviations from the typical spheroidal shape initially observed, small increases in particle diameter, and an apparent decrease in the optical density. In addition, use of the electron microscope at 75 kv resulted in some observable particle evaporation. Some particles eventually developed a halo-type structure such as shown in Fig. 10.

Number and Size Distribution of Collected Dust

Since the width of the impactor jet and the diameter of the electron microscope grids are both 3.0 mm, particles were deposited over the entire grid surface. Because of the characteristic non-uniformity of the impactor deposit pattern,

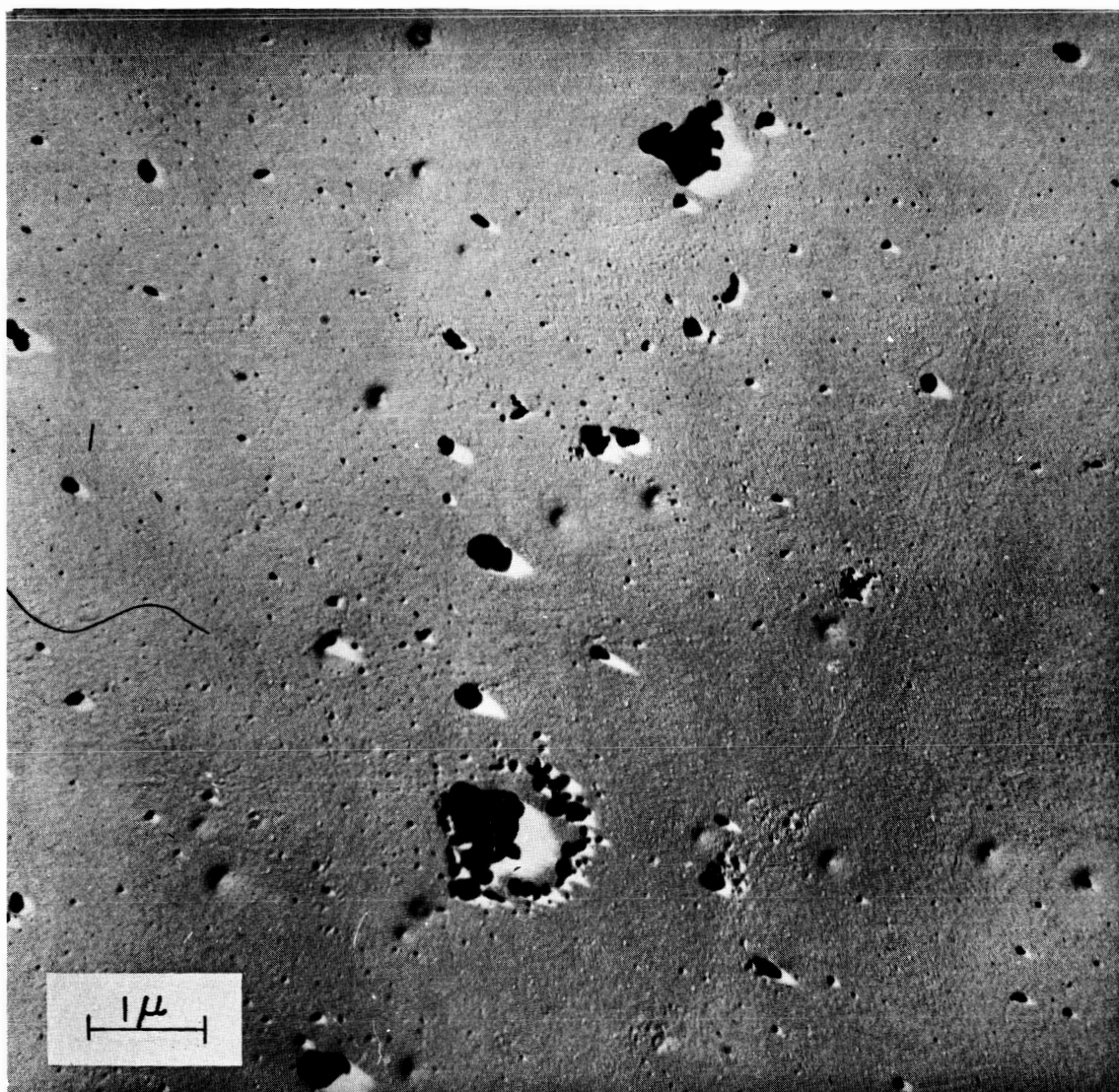


Fig. 10. Halo-Like Particle Produced by Exposure to Water Vapor

however, the number density of particles did vary as a function of distance from the center of the jet. For example, electron micrographs of a number of fields about 0.12 mm apart across the jet, show that the greatest deposit density occurred near the jet centerline. Lower concentrations were found under the jet edge. This distribution is shown in Fig. 11.

From electron micrographs of the three grid types, particles were counted and sized. As shown in Fig. 12, the distributions are reasonably consistent, and approximately log-normal. Measurements from each of a number of fields located near the center and edge of the particle deposit did not yield significant differences in size distribution that could be attributed to position of the field under the impactor jet.

A summary of the number mean diameters, geometric standard deviations and number density of particles collected on the three grid types is given in Table 4. For the following reasons, no particular significance is attached to the variation in values shown:

- 1) Uncertainty on the order of 10 percent in the accuracy of electron micrograph magnification.
- 2) Resolution losses on the oiled grids.
- 3) Differences in particle retention efficiency.

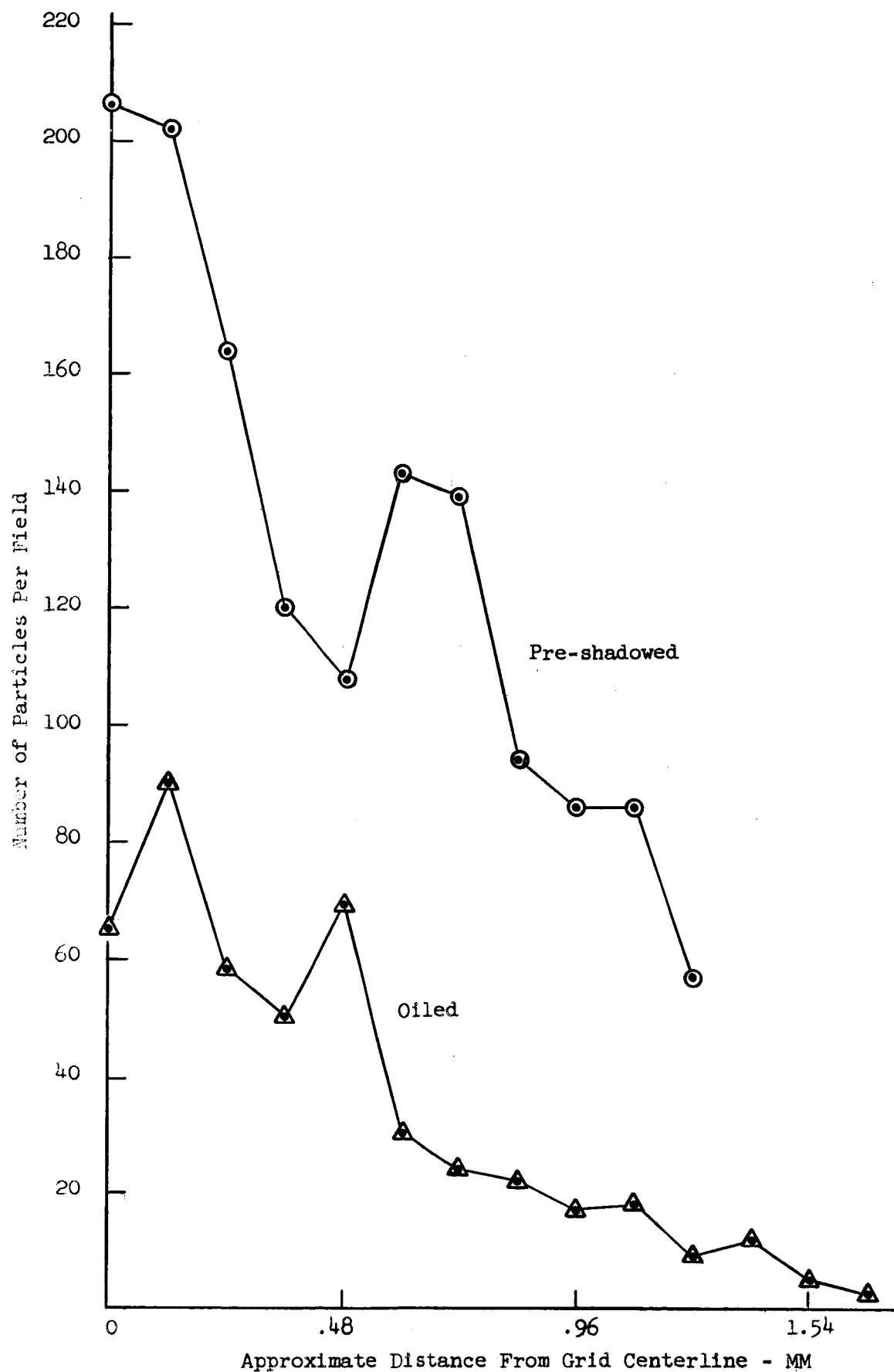


Fig. 11. Particle Number Density as a Function of Distance Across the Collection Surface

Legend:

- Type 1, dry formvar film
- ⊙ Type 2, formvar film, chromium pre-shadow
- ▲ Type 3, formvar film, 0.1 micron oil overlay

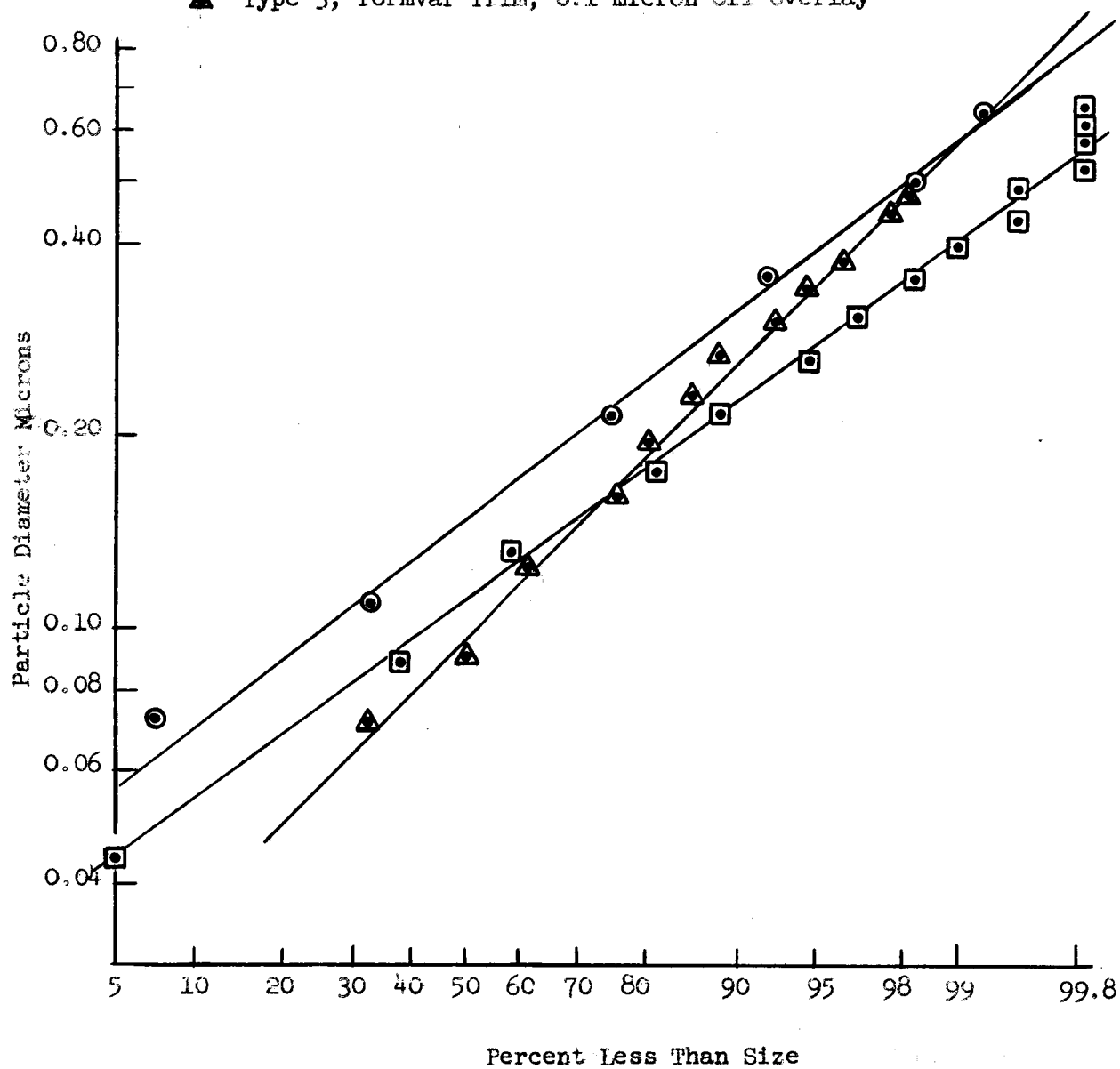


Fig. 12. Size Distribution of Particles Collected

Table 4. Particle Size Distribution

	Type 1 Formvar Surface	Type 2 Pre-Shadowed Surface	Type 3 Oiled Surface
Number mean diameter (microns)	0.112	0.15	0.098
Geometric standard deviation	1.75	1.80	2.17
Number density (per sq. mm)	4×10^5	3×10^5	2×10^5

8. Particle Analysis by Nuclear Magnetic Resonance

NMR studies were made in a Varian 12 in. magnet having tapered pole faces. The inhomogeneity of the magnetic field across the sample did not exceed 9.4 MG. This would amount to a broadening of the resonance line by 40 cycles. Measurements were made at 4.6 MHz using an NMR head developed at the Litton Applied Science Division. This unit has two sets of rf coils. The two sets are orthogonal, and are placed at right angles to the static magnetic field. One set of coils is used to apply the rotating rf field to the sample and the other picks up the induced voltage from the processing nuclei. The isolation between the input coils and the output coil is in excess of 150 dB when not in resonance. The input power to the coils is supplied from a Hewlett-Packard Type 606A signal generator through a balancing network. The output coil is connected into a matching network. The output of this feeds a receiver from which the IF output is used. A crystal diode supplies the potential to drive the y-axis of an x-y chart recorder. The x-axis drive voltage is supplied by the magnet power supply. The rate at which the magnet is swept over a range of field values is adjustable on the magnet power supply.

From calculations, we have concluded that a microgram of material

would be required to give a detectable signal. During checks for background signals we were able to detect copper in the rf coils and the presence of cobalt oxide in some glasswork. We believe that the equipment was operating at maximum sensitivity.

Tetramethyl silane in CDCl_3 was used as the zero reference, and calibration of frequency offset was effected by audio frequency modulation on the static magnetic field.

NMR spectroscopic analyses were conducted on Type 7 (dry) and, Type 8 oil coated films stripped from the glass slide base (see Section 3), and rolled into tight cylinders approximately 6 mm long, and 2 mm in diameter. Runs were made on control samples, and on samples exposed during the sampling interval. Since a complete spectrum analysis is extremely tedious, and beyond the scope of this program, the analysis was limited to a search for evidence of interactions involving the more abundant elements, such as silicon, iron, and nickel. Although definite spectra were obtained, we were not able to identify molecular structures associated with possible combinations of these elements.

The NMR scan revealed three definite resonances at frequencies typical of chelates, a complex type of metal-organic compound. The method for relating such results to a specific compound normally involves comparison of the resonant frequency patterns obtained by NMR, with published data from known materials. No data was found that could be correlated with the recorded spectrum, and the exact nature of the compounds detected is not known. The fact remains, however, that specific NMR resonances appeared in the collected sample that did not appear in control samples.

The foregoing resonances were found only in connection with analyses of oil coated substrates (Type 8). No resonances were found in tests with the

dry (Type 7) substrate. Since a chelate is an organic compound not normally expected in extraterrestrial debris, one may consider the rather tenuous possibility that the observed spectrum is derived from a reaction between the collected material and the oil substrate. We do not have sufficient data to support such an hypothesis.

In conclusion, the primary value of NMR spectroscopy appears to lie in establishing the molecular structure of compounds once the constituent elements have been ascertained by other means, such as electron microprobe spectroscopy.

9. Particle Studies with the Electron Mirror Microscope

Background

Because the Litton Electron Mirror Microscope (EMM) is a new analytical instrument, a brief description of this device is considered a desirable and appropriate preface to a discussion of work performed.

The EMM is principally a tool for the study of electric and magnetic fields associated with a specimen surface. Because the electrons which form the image do not interact physically with the specimen, it is basically a non-destructive method.

It should be understood that the EMM is not an electron transmission microscope nor a normal scanning beam electron microscope (often referred to as the SEM or Stereoscan). In the former, the electron beam passes through a thin specimen or a replica of the specimen surface. In the latter, a tight electron beam bombards the surface, creating secondary electrons and electron-induced conductivity with display on a cathode ray tube. In the EMM, electrons directed toward the specimen surface are reflected just before they reach the surface, and are then directed to a fluorescent screen where they depict the fields associated with the specimen surface.

The principle of operation is shown schematically in Fig. 13. The electron gun generates a beam of collimated electrons which are accelerated into the main EMM chamber. The magnetic prism deflects the electrons through a 15° angle and into the immersion objective lens. As the electrons pass through the final lens element they are de-accelerated by a strong retarding field of the order of 10^4 to 10^5 V/cm. This retarding field is the result of a 10 to 30 kV potential difference between the final element of the objective lens and the mirror specimen. Because the mirror specimen is negative with respect to

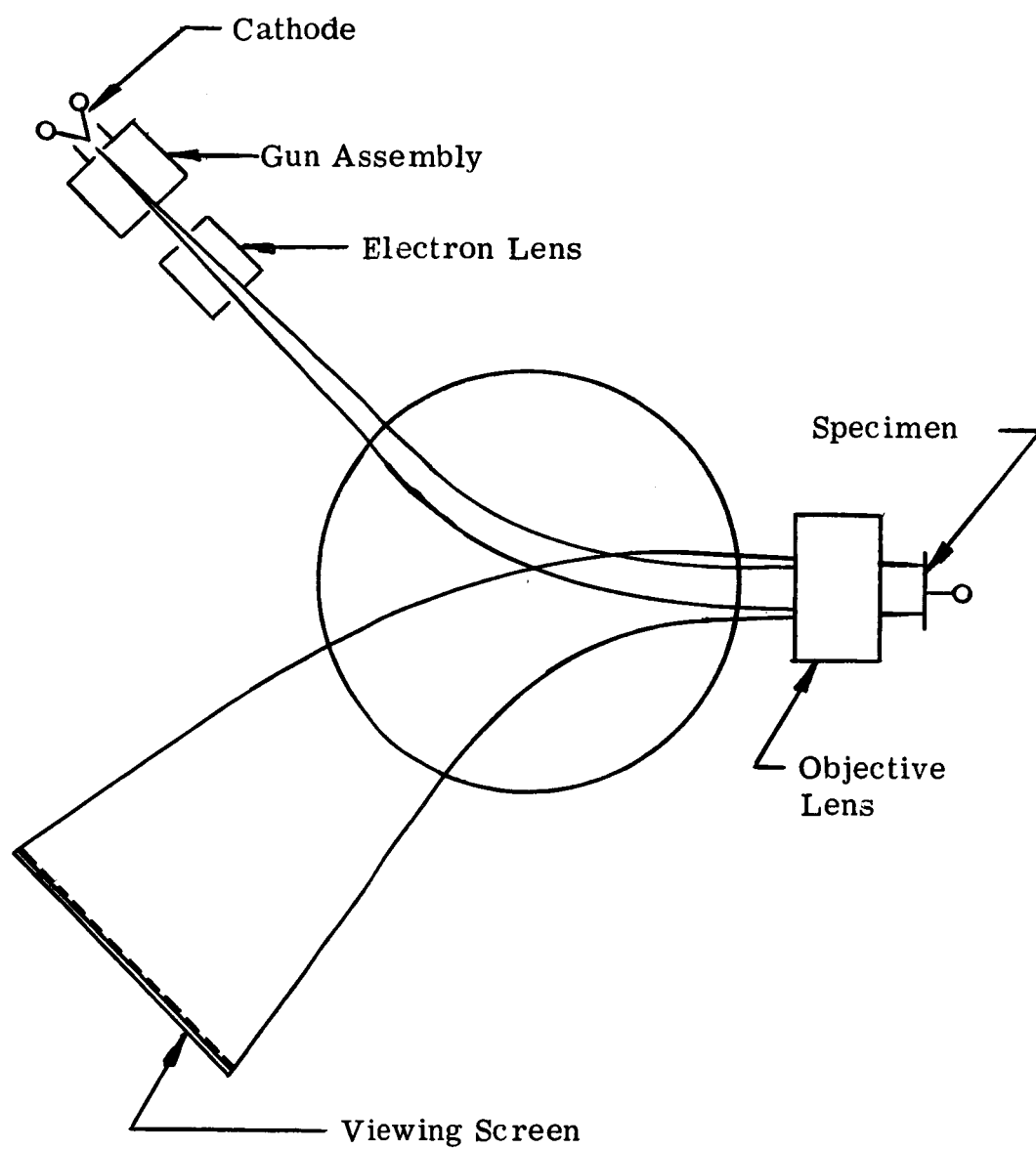


Fig. 13. Schematic of Y-type EMM.

the gun cathode, the electrons do not have enough energy to reach the specimen surface and are slowed to zero axial velocity at an electrical potential surface in front of the specimen. The electrons are then accelerated away from the specimen surface back through the immersion objective. The mirrored beam is deflected away from the incoming beam by the magnetic prism and directed onto a phosphor screen for visual observation or photographic record. A projector lens inserted in the path of the mirrored electrons can be used to further increase the magnification if so desired.

The unique aspect of electron mirror microscopy is that the electrons are mirrored from and interact with potential gradients or microfields near the specimen surface. It is the contours of the equipotential surfaces (i. e., potential gradients) which deflect the electrons and redistribute them in patterns observed as variations in image intensity at the phosphor screen. Because the electrons have very low kinetic energy at the point where they are interacting with the potential surfaces, very subtle variations in the contours can be detected. In particular, voltage differences as small as 20 mV and magnetic fields of less than 1 mG are within the present state-of-the-art.

With respect to particle studies, proper manipulation of the mirroring potential and beam position enables the operator to differentiate between conducting and non-conducting particles. He can also differentiate between magnetic and non-magnetic particles. If the particle is photo-sensitive its electrical response in the presence of light can be observed and related to the wavelength of incident energy that produced the response.

EMM Analysis of Collected Particles

In this work, most of the information was obtained by bombarding the particles with electrons from the beam and then observing secondary emission effects and charge dissipation effects. The latter is an indication of the electrical conductivity of the material. In interpreting the EMM microphotos obtained, it is important that several facts be understood:

- 1) Any contrast in these EMM microphotos indicates a change in electrical potential or a change in surface topology or a combination of both.
 - a) Any region that is whiter than its surroundings has a more positive potential than the surroundings or is a depression in the surface, or both.
 - b) Any region that is blacker than its surroundings is more negative than the surroundings or is a high spot on the surface, or both.
 - c) In some instances there is a dark spot surrounded by a white ring. Here the black spot is negative; the white ring denotes those electrons deflected away from the strongly negative region.
- 2) The size of a spot is not indicative of the size of the actual particle that causes the spot. The spot is much larger than the particle. The electron beam "sees" only the electrical microfield surrounding the particle. The size of the microfield depends on the amount of charge on the particle. At a minimum, the spot is about 5 times the size of the particle. The electrical field tends to smooth out any sharp physical variations in the shape of the particle.
- 3) Insulating particles can be charged negatively by bombardment with electrons. Electron energies of only a few volts are adequate for this purpose. Evidence of this charge-up condition is observed in the EMM as an increase in the diameter of the spot representing a given particle.

- 4) Even though a material is classed as an electrical insulator, it has a characteristic electrical conductivity. Different materials have different conductivities. In the EMM it is possible to charge up the particles, remove the bombarding electron beam, and observe the gradual discharge of the particles as gradual reduction in the size of the spots. This process classifies various types of materials without revealing their actual identity.
- 5) When most materials are bombarded with electrons they emit secondary electrons after the energy of the bombarding electrons has passed a certain threshold value. For many materials, this threshold is rather low--of the order of 15 eV. In (4) above, we explained that bombarding electrons increase the size of the black spots. This is true at low energies. As the bombarding energy is increased, the particles give up appreciable numbers of secondary electrons. These carry away negative charges from the particle, and if the rate of secondary emission exceeds the rate of negative buildup from the incident electrons, then the particle becomes positively charged and converts to a white spot on the screen. Since different materials exhibit different secondary electron emission characteristics, this secondary emission phenomenon identifies different species of particles.
- 6) Electron-induced conductivity is an additional phenomenon that must be considered in analyzing EMM data. The conductivity of many materials is increased when the material is bombarded with electrons--an effect most pronounced in oxides. In the case of the particles, this would mean that some charge would be leaking off while the net charge was becoming negative. This implies that some particles will charge up more slowly than others, and discharge more slowly after the beam is removed; a characteristic that varies with different materials.

From the foregoing, it can be recognized that the EMM observes the conductivity, secondary emission characteristics, and electron-generated conductivity of the particles. These properties all vary with temperature, thus providing a means of obtaining supporting clues in particle analysis.

EMM Particle Studies

As noted previously (Section 3), particles for EMM analysis were collected on 25 mm circular glass cover slips upon which a gold surface 0.1 microns thick had been evaporated. The gold is necessary as an electrical conductor to provide the mirroring potential.

All specimens were handled with care in a laminar flow dust-free hood. Fig. 14 is a typical EMM microphoto of a flight control surface. The dark spots are indicative of the levels of dust contamination observed.

Fig. 15 shows a typical region in the center of the impaction area on an oil-coated (Type 5) slide. The particle density is too great for particle examination.

Fig. 16 shows a region near the edge of the impaction area on an oil-coated slide. By comparison with similar regions on dry slides, it is evident that the oil film masks the small particles. No further examination of oil-coated slides was attempted.

Fig. 17 is a typical area in the center of the impaction region on a dry slide. The particle concentration is too great for detailed study of particles.

Fig. 18 is a field near the edge of the impaction area, where study of detailed particle behavior is possible. Here the only electron bombardment is the small amount resulting from the higher energy electrons in the beam. (An electron beam has a small spread in energy velocities.) A careful examination of many such areas revealed no conducting particles; all particles were insulators. The particle density in this region was of the order of 10^3 particles per mm^2 .

When the particles of Fig. 18 were bombarded with pulses of 10 V electrons, Fig. 19 resulted. The black spots depict particles that are charged

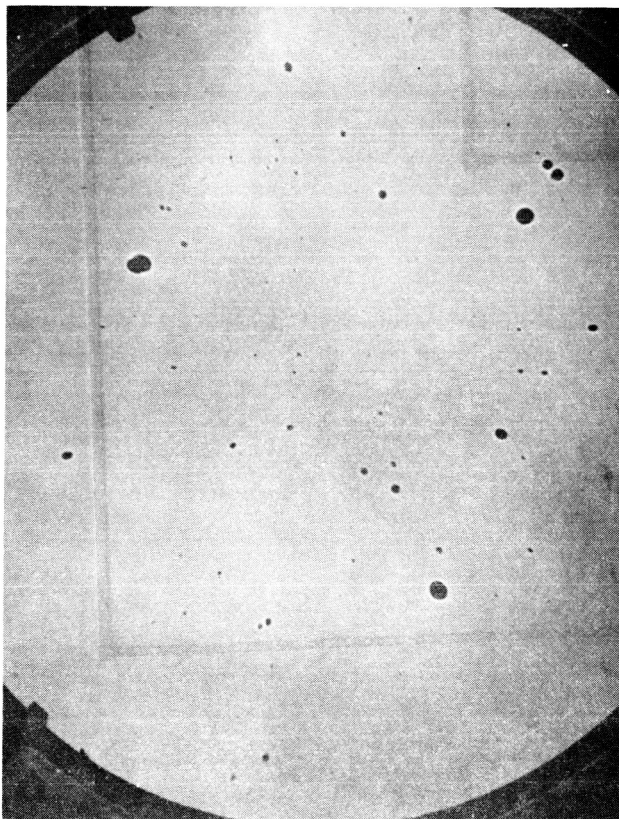


Fig. 14. EMM Microphoto of Flight Control Surface

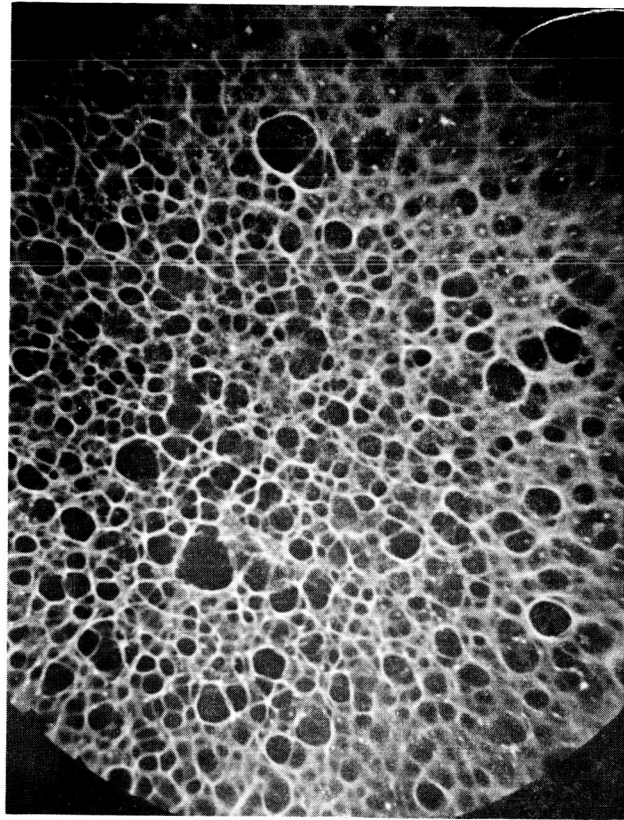


Fig. 15. EMM Microphoto, Center of Collection Area, Oil-Coated Slide

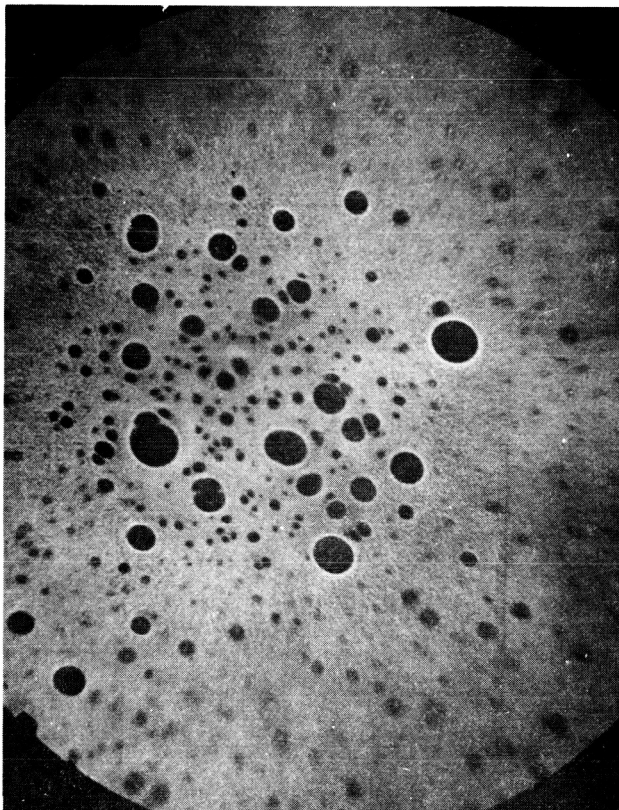


Fig. 16. EMM Microphoto, Edge of
Collection Area, Oil-Coated Slide

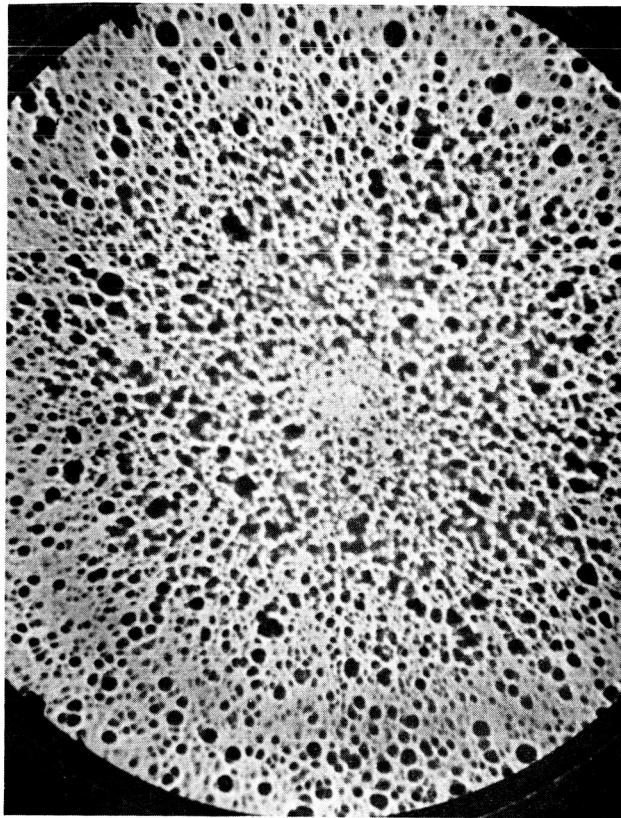


Fig. 17. EMM Microphoto, Center of
Impact Area, Dry Slide

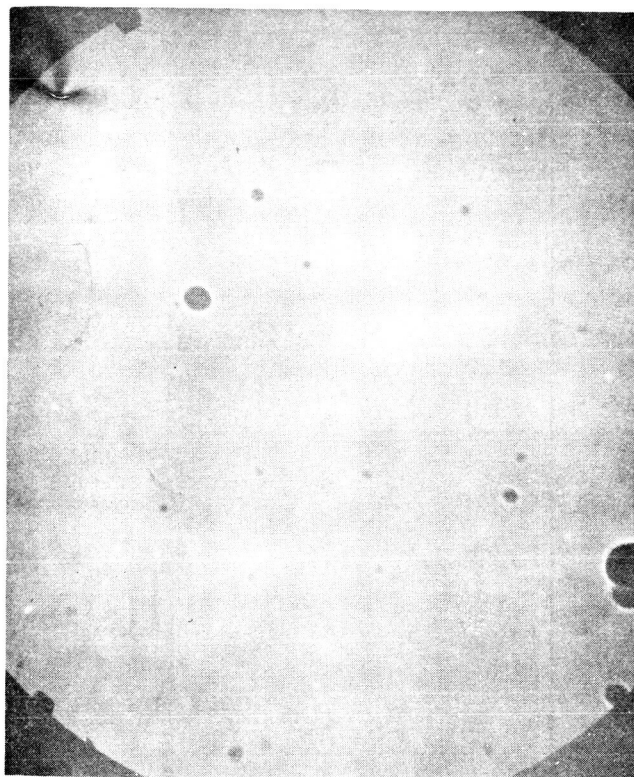


Fig. 18. EMM Microphoto, Edge of
Impaction Area, Dry Slide

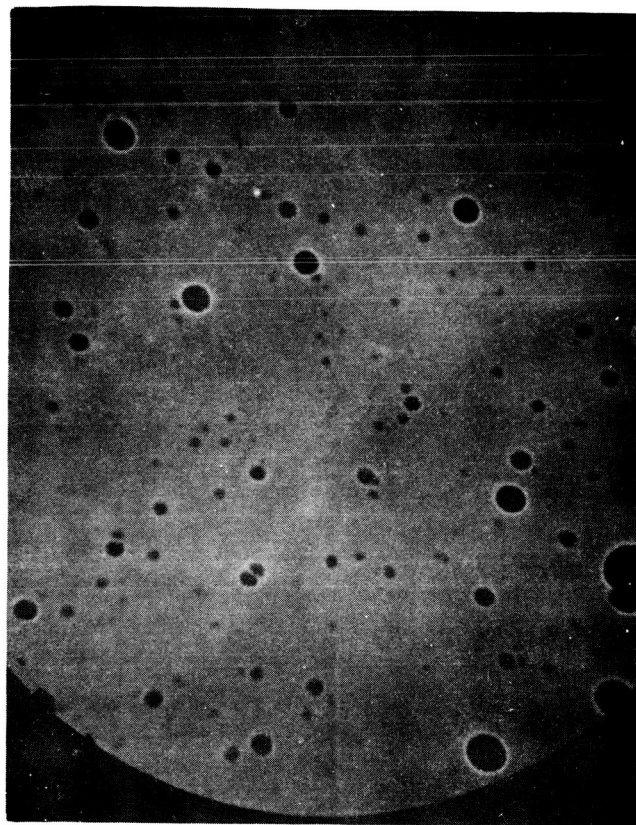


Fig. 19. Same Sample as Fig. 18; Particles
Bombarded with 10 eV Pulses

negatively by the impinging electrons. Here, the size of the spot is determined by the particle size and also by the rate at which the charge leaks off to the conducting surface of the glass slide.

As the electron bombardment voltage was further increased, a condition was reached as depicted in Fig. 20. Here, the white spots indicate that secondary electron emission is over-riding the negative charge build-up by electron bombardment, resulting in positively charged particles. This phenomenon occurred at about 15 V electron energy, which is typical of KCl or NaCl. A large number of particles have faded into the background, indicating a balance between negative charge storage and secondary electron emission.

In the progression of increasing electron bombardment voltages from Fig. 18 to Fig. 20, it was observed that some particles built up charge at rates different than others. This would indicate variations in electrical conductivity. Measurements of spot size indicate that 20% of the particles are of a different material than those included in the NaCl-KCl category above.

Electron microscope experiments with similar particles on specially prepared grids showed a marked change in the physical appearance of the particles after exposure to high humidity. Particles on gold-coated glass slides were given the same treatment and then examined in the EMM. No change in electrical behavior was observed.

Figures 21 through 26 show the effect of temperature on the particles through a range from 25⁰C to 350⁰C and back to 25⁰C. Heat was applied to the reverse side of the specimen slide by a resistance heater while the slide was in position in the EMM. Temperature of the slide was measured on the reverse side with a chromel-alumel thermocouple. Any given temperature was maintained steady until the electrical parameters of the particles had

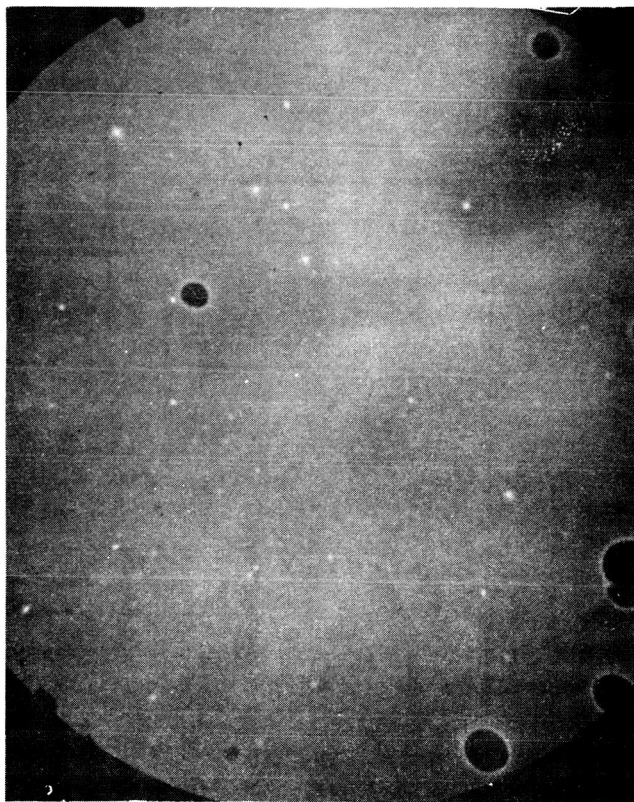


Fig. 20. Same Sample as Fig. 18; Particles
Bombarded with 15 eV Pulses

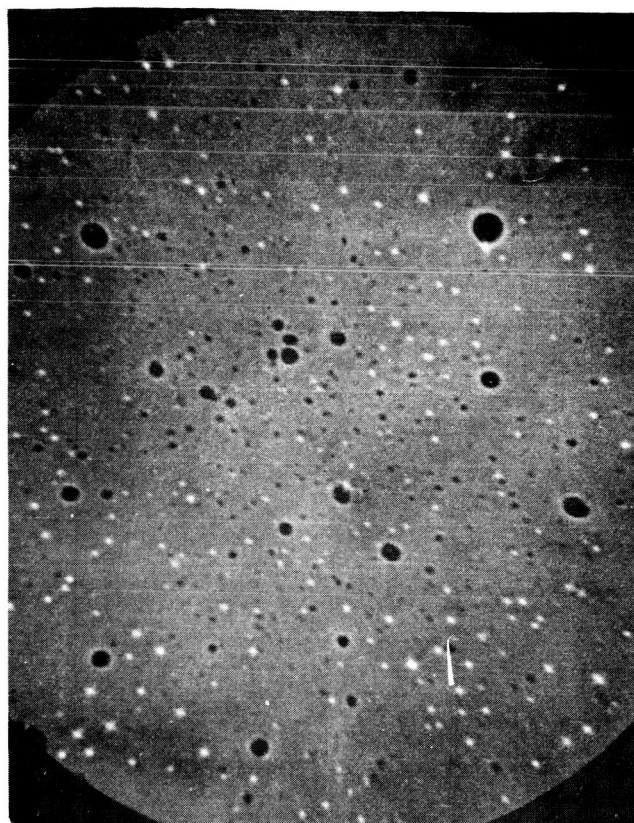


Fig. 21. Sample at 25°C; Particles
Bombarded with 40 eV Pulses

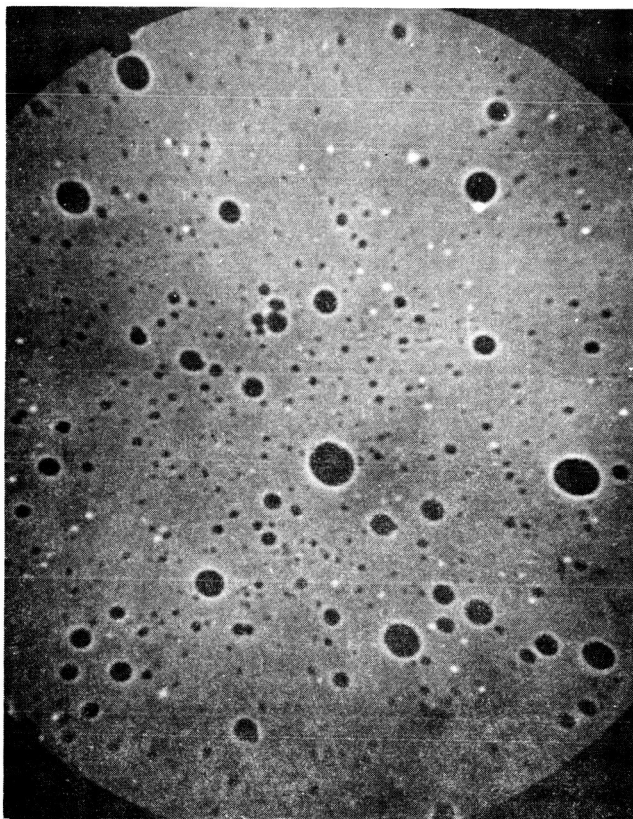


Fig. 22. Sample at 90°C; Particles
Bombarded with 40 eV Pulses

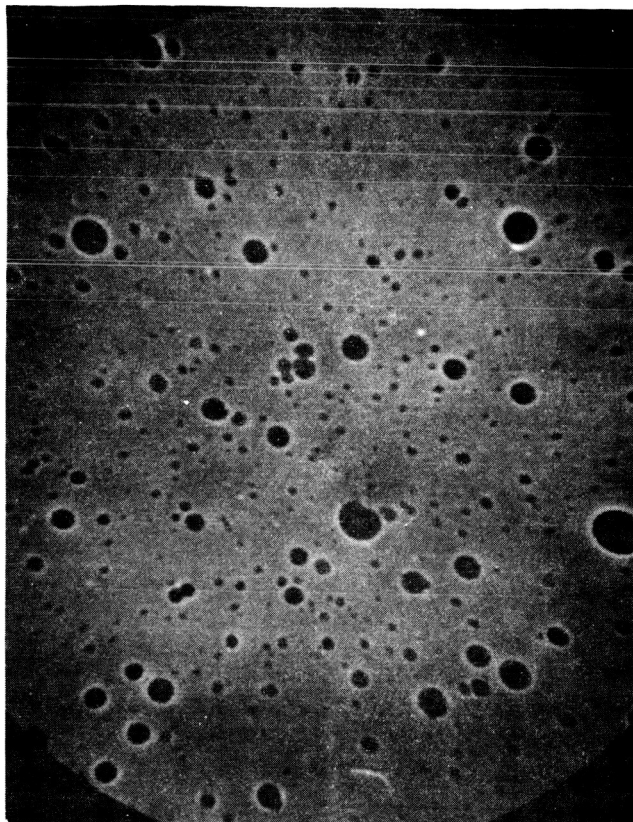


Fig. 23. Sample at 175°C; Particles
Bombarded with 40 eV Pulses

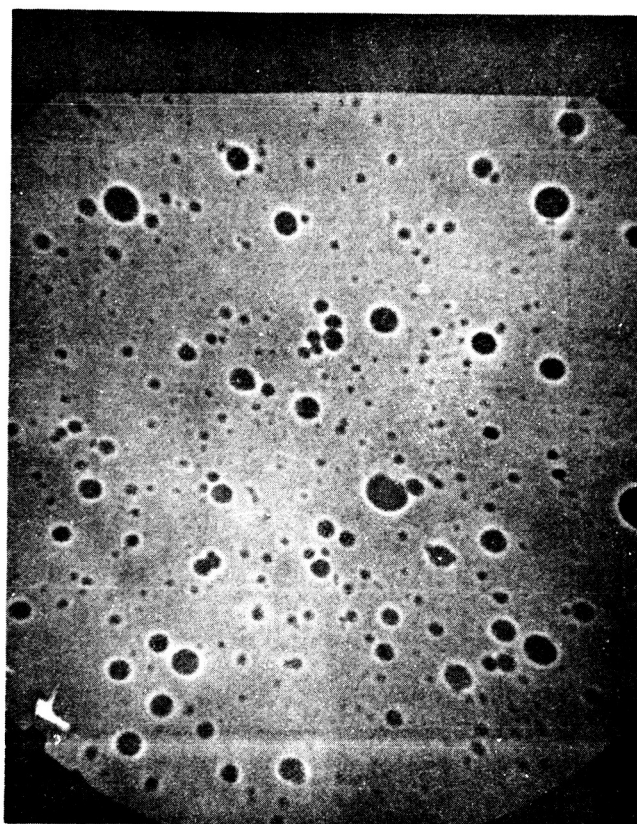


Fig. 24. Sample at 224°C; Particles
Bombarded with 40 eV Pulses

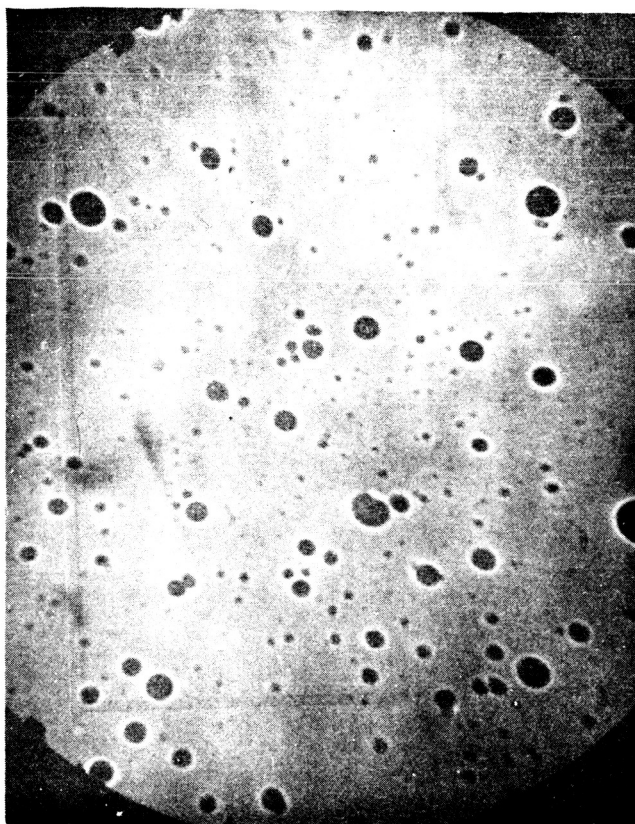


Fig. 25. Sample at 350°C; Particles
Bombarded with 40 eV Pulses

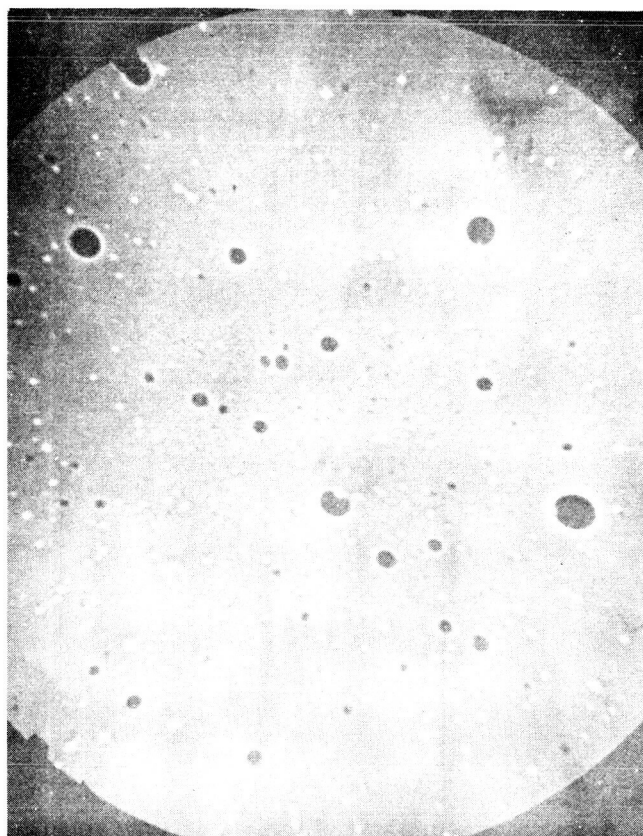


Fig. 26. After Cooling Back to 25°C ;
Particles Bombarded with 40 eV
Pulses

stabilized. It has been assumed that the temperature of the particles was the same as that measured by the thermocouple within $\pm 2^{\circ}\text{C}$. The electron bombarding energy in all cases was 40 V.

Fig. 21 is at 25°C , and shows a mixture of white positive particles and black negative particles. These are two different materials.

Fig. 22, at 90°C , shows a general increase of particle sensitivity or a decrease in secondary emission, depicted as an increase in size of some black spots and a conversion of most white spots to black. Several white spots became more intense, indicating increased secondary electron emission. These few particles are probably different material.

At 175°C , Fig. 23, secondary emission has decreased, and in some cases resistivity has decreased.

A halo effect around some of the particles is noticeable at 225°C , Fig. 24. This is still more pronounced at 350°C , Fig. 25. The physical basis for this halo is not yet understood. It is more pronounced for some particles than for others. The halo disappears on cooling.

The various physical changes observed in this experiment can be repeated. With detailed study they can be used to differentiate among particles, and in many instances may relate the particles to specific classes of material.

Fig. 26 shows the sample after cooling for 14 hours in vacuum. A comparison with the sample before heating, Fig. 21, shows a slight decrease in secondary emission or increase in resistivity. This is probably due to the removal of water of crystallization at the higher temperature.

All EMM investigations were made in a vacuum in the 1 to 5×10^{-6} Torr range.

The EMM examination appeared to be non-destructive. Residual gas ions bombard the sample in only one spot, and therefore, have little effect on the particles. Maximum electron bombardment was 50 V.

One unknown quantity in the examination of such particles is the nature of the electrical contact which the particle makes with the substrate; very little is known or understood about the electrical contacts made by sub-micron particles. We have initially assumed that separation distances are so small that conduction is reasonably good. Further study in this area is desirable.

Conclusions, EMM Study

This initial study using the Electron Mirror Microscope may be characterized as a preliminary investigation of the method as a means for deriving information from observed electrical and magnetic characteristics of the particles. While the scope of effort did not permit detailed analysis of data in depth, the following general conclusions are believed valid:

- 1) No electrically conducting particles were observed.
- 2) No magnetic particles were detected. This observation is tempered by the knowledge that a very small percentage of magnetic particles may have been overlooked because of their low ratio to other particles.
- 3) Since cycling to 350⁰C did not appreciably change the electrical nature of the particles, it is assumed that no organic material was present.
- 4) No photoresponsive oxides were observed. Tests were limited to those materials that would be excited above the quartz cutoff for ultraviolet light.
- 5) Storage in a humid atmosphere had no observable effect on the charge acceptance, conductivity, or secondary emission coefficient of the particles.

- 6) Electrical discharge rates indicate that most of the particles collected were of two types. The balance of the particles appear to represent a variety of materials.
- 7) Some particles emitted secondary electrons at 15 eV. Others gave no evidence of strong emission at 40 eV. This tends to support the argument for two major categories of particles.
- 8) Heat reduced the evidence of secondary emission. This was attributed to an increase in conductivity of the particles. The effect was noted at two temperature levels corresponding to two threshold levels of secondary emission.

10. Electron Microprobe Analysis

About midway in the program, an additional opportunity for particle analysis became available through use of MAC, Model 400* an electron microprobe analyzer located in the Geology Department at the University of Minnesota.

Initial tests using samples collected on gold-coated microscope cover slips (Type 4 substrates) gave negative results. This was attributed to the low mass of particles in the electron beam. It was subsequently revealed that a sample fraction given to Dr. Michael Carr of the U. S. Geological Survey, Menlo Park, California, had been subjected to microprobe analysis, independently, with similar negative results.

Later in the program, a technique being developed** by another group within the Applied Science Division, was employed to gather and concentrate a mass of particles sufficient for analysis. A spectrum scan of the concentrated sample yielded positive evidence of three elements:

<u>Element</u>	<u>Characteristic Emmission Lines Detected</u>
Potassium	$K\alpha$, $K\beta$
Chlorine	$K\alpha$, $K\beta$
Lead	$L\alpha$, $M\alpha$, $M\beta$

A second examination, using a much larger sample transferred to a copper substrate, confirmed this result. Although quantitative interpretations were not attempted, the X-ray lines were strong and unmistakable. There was no evidence indicating the presence of silicon, iron, nickle, sulfur or sodium.

*Materials Analyses Company

**This technique is to be described in the open literature at a later date.

II. Discussion of Results

While it is not inconceivable that potassium, lead and chlorine could be present in the stratosphere, the absence of other, more abundant elements, raises a serious question as to the validity of the sample collected. As previously noted in the introduction and summary, potassium chlorate and lead nitrate were found to be components of the charge used in a squib actuator fired at termination. (Although we are aware that potassium and chlorine are also elemental constituents of some solid-fuel rocket formulations, this is rejected as offering a rather tenuous and unlikely possibility.)

Inspection of electron micrographs does not reveal any characteristic differences within the particle population that might serve to differentiate between squib products and particles that might be of stratospheric or extra-terrestrial origin. In view of the fact that the microprobe analyses reveal only elements known to be present in the squib charge, we have assumed that an unknown but major fraction of the collected sample is contamination.

It may be pointed out that this experiment has involved a first test of a previously untried system. On future flights, minor modifications of the control system and actuators will eliminate the problem of squib contamination.

A review of engineering factors and flight performance data also indicates that on subsequent tests it will be possible to sample over 700,000 cubic feet of air at 40 km--a substantial increase over the volume processed on this first flight.

12. References

- Davies, C. N. and M. Aylward. The trajectories of heavy solid particles in a two-dimensional jet of ideal fluid impinging normally upon a plate. Proc. Phys. Soc. (London) 64B: 889-911 (1951).
- Junge, C. E., C. W. Chagnon and J. E. Manson. Stratospheric aerosols. J. Meteorol. 18: 81-108 (1961).
- McFarland, A. R. and H. W. Zeller. Study of a large volume impactor for high altitude aerosol collection. Final report, Contract AT(11-1)-401 (1963).
- Ranz, W. E. and J. B. Wong. Impaction of dust and smoke particles on surface and body collectors. Ind. Eng. Chem. 44: 1371-81 (1952).
- Stern, S. C., H. W. Zeller and A. I. Schekman. Collection efficiency of jet impactors at reduced pressures. Ind. Eng. Chem. Fundamentals 1: 273-77 (1962).
- Wood, R. C., R. K. Olson and A. R. McFarland. Air ejector filter sampler: A balloon-borne collector of radioactive stratospheric debris. J. App. Met. 5: 866-871 (1966).